Computational Geosciences (2023) 27:687–705
https://doi.org/10.1007/s10596-023-10226-1

ORIGINAL PAPER

High-order compact difference schemes based on the local one-dimensional method for high-dimensional nonlinear wave equations

Mengling Wu[1,2] · Zhi Wang[2] · Yongbin Ge[1]

Received: 27 August 2022 / Accepted: 25 May 2023 / Published online: 14 July 2023

Abstract
In this paper, two compact difference schemes are established for solving two-dimensional (2D) and three-dimensional (3D) nonlinear wave equations with variable coefficients, respectively, by using the local one-dimensional (LOD) method and the fourth-order compact difference approximation formulas of the second-order derivatives. Firstly, a four-step fourth-order compact scheme is derived to solve the 2D nonlinear wave equation. The stability of the scheme 2for solving the linear equation is analyzed by the discrete Fourier method, which shows that it is conditionally stable. Then, the method is extend to solve the 3D nonlinear wave equation and stability condition for the linear equation is also analyzed. Finally, numerical experiments are conducted to verify the accuracy and stability of the proposed schemes.

Keywords High-dimensional nonlinear wave equation · Variable coefficient · Local one-dimensional · Fourth-order compact scheme

1 Introduction

The wave equation is a type of hyperbolic differential equation, which can describe the propagation of waves in the atmosphere and is widely used in elasticity, geophysics and other fields. The numerical solution of wave equation is the basis of reverse time migration and plays an important role in seismic wave propagation, full wave inversion and seismic imaging. Therefore, it is of great practical significance to seek for the numerical solution of wave equation [1–3].

Among the available numerical methods, finite difference method is widely used because of its convenience and easy implementation. It is worth noting that the high-order compact (HOC) difference method has attracted the interest of many seismic modeling researchers, which not only has high accuracy but also can effectively suppress the numerical dispersion [4–7]. Compared to the noncompact difference schemes [8, 9], the compact difference schemes require smaller mesh stencil, which is simpler and more convenient in dealing with boundary conditions. It is well-known that difference schemes include explicit difference schemes and implicit difference schemes. The explicit difference schemes are limited by more stringent stability conditions, so usually the temporal step size must be very small, which results in longer computational times [10–12]. On the contrary, due to more flexible stability condition, implicit difference schemes have attracted much attention [13–20]. For instance, for the nonlinear wave equation with damping function, Li and Sun [16] derived a family of linearly implicit difference schemes based on scalar auxiliary variable technique with a combination of classical high-order Gauss methods and extrapolation. For the sine-Gordon equation, Su [19] considered a localized scheme of approximate analytical solutions. For the Klein-Gordon equation, Liu and Wu [18] explored

✉ Yongbin Ge
gybnxu@yeah.net

Mengling Wu
wuml2019@126.com

Zhi Wang
wangzhi11@yeah.net

[1] School of Science, Dalian Minzu University, Dalian 116600, China

[2] Institute of Applied Mathematics and Mechanics, Ningxia University, Yinchuan 750021, China

arbitrarily-order implicit schemes based on the operator spectrum theory. However, implicit difference schemes for solving high-dimensional equations usually produce large sparse linear systems at each time step, which usually has to be solved by certain iterative method with a relatively large calculation cost.

In order to overcome the shortcoming of the above implicit difference methods, many researchers tend to employ splitting techniques, such as the alternating direction implicit (ADI) and the LOD methods. By these two ways, the high-dimensional problems can be transformed into several one-dimensional problems, which can improve computational efficiency and save storage space [21]. Many ADI methods have been successfully applied to the numerical solutions of nonlinear wave equations. For example, Ref. [22] introduced a nonlinear ADI scheme and a linear ADI scheme, both of which have $O(\tau^4 + h^4)$ accuracy for solving the 2D Klein-Gordon and sine-Gordon equations. Ref. [23] established two compact ADI schemes with $O(\tau^2 + h^4)$ for solving the 2D and 3D viscous nonlinear wave equations. For more details on the ADI schemes, readers are referred to Refs. [6, 24–27]. Until now, the LOD methods have been mainly applied to solve the homogeneous linear wave equations [28–31]. For example, Ref. [28] proposed a conditionally stable difference scheme with $O\left(\tau^4 + h^4\right)$ based the LOD method to solve the 2D linear problem. Whereafter, the method was extended to solve the 3D linear problem [29]. Ref. [31] introduced a Runge-Kutta scheme combined with the LOD method. In addition, for the 3D nonhomogeneous linear wave equation, Ref. [32] described a fourth-order implicit scheme based on the LOD method. Since it requires solving large sparse linear systems, it increases the computational complexity. Therefore, in this paper, we are dedicated to develop a compact high-order LOD method to find the numerical solutions of the 2D and 3D nonlinear wave equations with variable coefficients. Compared to the methods in Refs. [28–32], the presented method can not only be used to solve nonlinear high-dimensional wave equations, but also has smaller computational error. In addition, our method has better stability and a relatively large time step size can be used to reduce the total number of time advancing steps in the calculation process.

Other parts of this article are arranged as follows. In Section 2, for the 2D nonlinear wave equation, the new implicit compact scheme and stability analysis are introduced. In Section 3, the method is extended to the 3D nonlinear wave equation. In Section 4, the numerical experiments are conducted to prove the theoretical analysis. In Section 5, the conclusion is drawn.

2 2D nonlinear wave equation

Considering the 2D nonlinear wave equations with variable coefficients as follows

$$\frac{\partial^2 u(X,t)}{\partial t^2} = v^2(X)\Delta u(X,t) + f(u(X,t)), \quad (X,t) \in \Omega \times (0,T], \tag{1}$$

with the initial conditions

$$u(X,0) = \varphi(X), \quad \frac{\partial u(X,0)}{\partial t} = \psi(X), \quad X \in \bar{\Omega}, \tag{2}$$

and the boundary conditions

$$u(X,t) = g(X,t), \quad (X,t) \in \partial\Omega \times (0,T], \tag{3}$$

where $\Omega = (d_1, d_2)^2 \in \mathbb{R}^2$, d_1, d_2 are constants and $d_1 < d_2$. $\partial\Omega$ is the boundary of Ω and $\bar{\Omega} = \Omega \cup \partial\Omega$. $(0, T]$ is the time region. Δ is the Laplace operator. $X = (x, y)$ is spatial variable, $v(X)$ is the wave velocity, $f(u(X,t))$ is the nonlinear source term. $\varphi(X)$, $\psi(X)$ and $g(X,t)$ are known sufficiently smooth functions and their high-order derivatives exist. Further, when $f(u(X,t))$ is replaced by $\sin(u)$ or $\sinh(u)$, Eq. (1) is reduced to the sine-Gordon equation [17] or sinh-Gordon equation [33]. When $f(u(X,t))$ is replaced by $u + u^k$, Eq. (1) is referred to as the Klein-Gordon equation [18].

To build a difference scheme, we divide the definition domain (d_1, d_2) into N subintervals with the spatial grid size $h = \frac{d_2 - d_1}{N}$. The temporal step size is $\tau = \frac{T}{M}$. The grid points are denoted as $\left(x_i, y_j, t_n\right)$, in which, $x_i = d_1 + ih, y_j = d_1 + jh, t_n = n\tau, i, j = 0, 1, \cdots, N, n = 0, 1, \cdots, M$.

Letting $w^2(x,y) = \frac{1}{v^2(x,y)}$, the LOD technique [35] is applied to split the 2D problem (1) as follows

$$\frac{1}{2}w^2(x,y)\frac{\partial^2 u}{\partial t^2} = \frac{\partial^2 u}{\partial x^2} + \frac{1}{2}w^2(x,y)f(u), \tag{4}$$

$$\frac{1}{2}w^2(x,y)\frac{\partial^2 u}{\partial t^2} = \frac{\partial^2 u}{\partial y^2} + \frac{1}{2}w^2(x,y)f(u). \tag{5}$$

2.1 Implicit compact difference scheme

Firstly, we consider Eq. (4) at grid point $\left(x_i, y_j, t_n\right)$, i.e.,

$$\frac{1}{2}w_{i,j}^2\left(\frac{\partial^2 u}{\partial t^2}\right)_{i,j}^n = \left(\frac{\partial^2 u}{\partial x^2}\right)_{i,j}^n + \frac{1}{2}w_{i,j}^2 f(u_{i,j}^n). \tag{6}$$

In Eq. (6), the $\frac{\partial^2 u}{\partial t^2}$ and $\frac{\partial^2 u}{\partial x^2}$ are discretized by the fourth-order compact difference method [34]

$$\begin{aligned}&\frac{1}{2}w_{i,j}^2\left(1+\frac{(\tau/2)^2}{12}\delta_t^2\right)^{-1}\delta_t^2 u_{i,j}^n \\ &=\left(1+\frac{h^2}{12}\delta_x^2\right)^{-1}\delta_x^2 u_{i,j}^n+\frac{1}{2}w_{i,j}^2 f(u_{i,j}^n)+O\left(\tau^4+h^4\right),\end{aligned} \tag{7}$$

in which,

$$\begin{aligned}\delta_x^2 u_{i,j}^n &= \frac{u_{i+1,j}^n-2u_{i,j}^n+u_{i-1,j}^n}{h^2}, \\ \delta_t^2 u_{i,j}^n &= \frac{u_{i,j}^{n+\frac{1}{2}}-2u_{i,j}^n+u_{i,j}^{n-\frac{1}{2}}}{(\tau/2)^2}.\end{aligned} \tag{8}$$

Noticing that the high-order term $\left(\frac{h^2}{12}\delta_x^2\cdot\frac{(\tau/2)^2}{12}\delta_t^2\right)w_{i,j}^2 f(u_{i,j}^n)$ is a high-order truncation error term, i.e., $O\left(\tau^2h^2\right)$, Eq. (7) can be rewritten as

$$\begin{aligned}&\left(1+\frac{h^2}{12}\delta_x^2\right)w_{i,j}^2\left[\frac{u_{i,j}^{n+\frac{1}{2}}-2u_{i,j}^n+u_{i,j}^{n-\frac{1}{2}}}{(\tau/2)^2}\right] \\ &=2\delta_x^2\left(\frac{1}{12}u_{i,j}^{n+\frac{1}{2}}+\frac{5}{6}u_{i,j}^n+\frac{1}{12}u_{i,j}^{n-\frac{1}{2}}\right)+\frac{2w_{i,j}^2}{3}f(u_{i,j}^n) \\ &\quad+\frac{1}{12}\left[w_{i+1,j}^2 f(u_{i+1,j}^n)+w_{i-1,j}^2 f(u_{i-1,j}^n)\right] \\ &\quad+\frac{w_{i,j}^2}{12}\left[f(u_{i,j}^{n+\frac{1}{2}})+f(u_{i,j}^{n-\frac{1}{2}})\right]+O\left(\tau^4+\tau^2h^2+h^4\right).\end{aligned} \tag{9}$$

Omitting $O\left(\tau^4+\tau^2h^2+h^4\right)$, letting $\lambda=\tau/h$, and multiplying both sides of Eq. (9) by $\frac{\tau^2}{2}$, i.e.,

$$\begin{aligned}&\left(\frac{5w_{i,j}^2}{3}+\frac{\lambda^2}{6}\right)u_{i,j}^{n+\frac{1}{2}}+\left(\frac{w_{i+1,j}^2}{6}-\frac{\lambda^2}{12}\right)u_{i+1,j}^{n+\frac{1}{2}} \\ &\quad+\left(\frac{w_{i-1,j}^2}{6}-\frac{\lambda^2}{12}\right)u_{i-1,j}^{n+\frac{1}{2}} \\ &=\left(\frac{10w_{i,j}^2}{3}-\frac{5\lambda^2}{3}\right)u_{i,j}^n+\left(\frac{w_{i+1,j}^2}{3}+\frac{5\lambda^2}{6}\right)u_{i+1,j}^n \\ &\quad+\left(\frac{w_{i-1,j}^2}{3}+\frac{5\lambda^2}{6}\right)u_{i-1,j}^n-\left(\frac{5w_{i,j}^2}{3}+\frac{\lambda^2}{6}\right)u_{i,j}^{n-\frac{1}{2}} \\ &\quad-\left(\frac{w_{i+1,j}^2}{6}-\frac{\lambda^2}{12}\right)u_{i+1,j}^{n-\frac{1}{2}}-\left(\frac{w_{i-1,j}^2}{6}-\frac{\lambda^2}{12}\right)u_{i-1,j}^{n-\frac{1}{2}} \\ &\quad+\frac{w_{i,j}^2\tau^2}{3}f(u_{i,j}^n)+\frac{\tau^2}{24}\Big[w_{i+1,j}^2 f(u_{i+1,j}^n) \\ &\quad+w_{i-1,j}^2 f(u_{i-1,j}^n)\Big]+\frac{w_{i,j}^2\tau^2}{24}\left[f(u_{i,j}^{n+\frac{1}{2}})+f(u_{i,j}^{n-\frac{1}{2}})\right].\end{aligned} \tag{10}$$

Equation (10) is a fourth-order compact difference scheme for solving Eq. (6).

Similarly, we consider Eq. (5) at the grid point $(x_i, y_j, t_{n+\frac{1}{2}})$, i.e.,

$$\frac{1}{2}w_{i,j}^2\left(\frac{\partial^2 u}{\partial t^2}\right)_{i,j}^{n+\frac{1}{2}}=\left(\frac{\partial^2 u}{\partial y^2}\right)_{i,j}^{n+\frac{1}{2}}+\frac{1}{2}w_{i,j}^2 f(u_{i,j}^{n+\frac{1}{2}}). \tag{11}$$

Using similar method, we can obtain a fourth-order compact difference scheme for solving Eq. (11) as follows

$$\begin{aligned}&\left(\frac{5w_{i,j}^2}{3}+\frac{\lambda^2}{6}\right)u_{i,j}^{n+1}+\left(\frac{w_{i,j+1}^2}{6}-\frac{\lambda^2}{12}\right)u_{i,j+1}^{n+1} \\ &+\left(\frac{w_{i,j-1}^2}{6}-\frac{\lambda^2}{12}\right)u_{i,j-1}^{n+1}=\left(\frac{10w_{i,j}^2}{3}-\frac{5\lambda^2}{3}\right)u_{i,j}^{n+\frac{1}{2}} \\ &+\left(\frac{w_{i,j+1}^2}{3}+\frac{5\lambda^2}{6}\right)u_{i,j+1}^{n+\frac{1}{2}}+\left(\frac{w_{i,j-1}^2}{3}+\frac{5\lambda^2}{6}\right)u_{i,j-1}^{n+\frac{1}{2}} \\ &-\left(\frac{5w_{i,j}^2}{3}+\frac{\lambda^2}{6}\right)u_{i,j}^n-\left(\frac{w_{i,j+1}^2}{6}-\frac{\lambda^2}{12}\right)u_{i,j+1}^n \\ &-\left(\frac{w_{i,j-1}^2}{6}-\frac{\lambda^2}{12}\right)u_{i,j-1}^n+\frac{w_{i,j}^2\tau^2}{3}f(u_{i,j}^{n+\frac{1}{2}}) \\ &+\frac{\tau^2}{24}\left[w_{i,j+1}^2 f(u_{i,j+1}^{n+\frac{1}{2}})+w_{i,j-1}^2 f(u_{i,j-1}^{n+\frac{1}{2}})\right] \\ &+\frac{w_{i,j}^2\tau^2}{24}\left[f(u_{i,j}^{n+1})+f(u_{i,j}^n)\right].\end{aligned} \tag{12}$$

Equations (10) and (12) are HOC difference scheme based on the LOD method (HOC-LOD) for solving Eq. (1). Its truncation error is $O\left(\tau^4+\tau^2h^2+h^4\right)$, which means the scheme has the fourth-order accuracy. As the HOC-LOD scheme is a four-step scheme, it requires to compute the values of $u_{i,j}^{\frac{1}{2}}$ and $u_{i,j}^1$ in advance. The computational method is given in the following part.

2.2 Computation of the start-up time steps

By Taylor expansions, we have that

$$u_{i,j}^{\frac{1}{2}}=u_{i,j}^0+\frac{\tau}{2}\left(\frac{\partial u}{\partial t}\right)_{i,j}^0+\frac{\tau^2}{8}\left(\frac{\partial^2 u}{\partial t^2}\right)_{i,j}^0+\frac{\tau^3}{48}\left(\frac{\partial^3 u}{\partial t^3}\right)_{i,j}^0$$

$$+\frac{\tau^4}{384}\left(\frac{\partial^4 u}{\partial t^4}\right)_{i,j}^0+O\left(\tau^5\right), \tag{13}$$

$$u_{i,j}^1=u_{i,j}^0+\tau\left(\frac{\partial u}{\partial t}\right)_{i,j}^0+\frac{\tau^2}{2}\left(\frac{\partial^2 u}{\partial t^2}\right)_{i,j}^0+\frac{\tau^3}{6}\left(\frac{\partial^3 u}{\partial t^3}\right)_{i,j}^0 +\frac{\tau^4}{24}\left(\frac{\partial^4 u}{\partial t^4}\right)_{i,j}^0+O\left(\tau^5\right). \tag{14}$$

For simplicity, we mark the functions as follows

$$\begin{array}{llll}\frac{\partial\xi}{\partial x}=\xi_x, & \frac{\partial\xi}{\partial y}=\xi_y, & \frac{\partial^2\xi}{\partial x^2}=\xi_{xx}, & \frac{\partial^2\xi}{\partial y^2}=\xi_{yy},\\ \frac{\partial^3\xi}{\partial x^3}=\xi_{xxx}, & \frac{\partial^3\xi}{\partial xy^2}=\xi_{xyy}, & \frac{\partial^3\xi}{\partial x^2 y}=\xi_{xxy}, & \frac{\partial^3\xi}{\partial y^3}=\xi_{yyy},\\ \frac{\partial^4\xi}{\partial x^4}=\xi_{xxxx}, & \frac{\partial^4\xi}{\partial x^2y^2}=\xi_{xxyy}, & \frac{\partial^4\xi}{\partial y^4}=\xi_{yyyy}, & \end{array}$$

here, ξ represents for φ, w^2 and ψ.

By Eqs. (1) and (2), we can get that

$$\begin{aligned}\left(\frac{\partial^2 u}{\partial t^2}\right)_{i,j}^0&=\frac{1}{w_{i,j}^2}\left(\frac{\partial^2 u}{\partial x^2}+\frac{\partial^2 u}{\partial y^2}\right)_{i,j}^0+f(u)_{i,j}^0\\&=\frac{1}{w_{i,j}^2}\left(\varphi_{xx}+\varphi_{yy}\right)_{i,j}+f(u)_{i,j}^0,\end{aligned} \tag{15}$$

$$\begin{aligned}\left(\frac{\partial^3 u}{\partial t^3}\right)_{i,j}^0&=\frac{\partial}{\partial t}\left(\frac{\partial^2 u}{\partial t^2}\right)_{i,j}^0\\&=\frac{1}{w_{i,j}^2}\left[\left(\frac{\partial^2}{\partial x^2}+\frac{\partial^2}{\partial y^2}\right)\left(\frac{\partial u}{\partial t}\right)_{i,j}^0\right]+\left[\frac{\partial f(u)}{\partial t}\right]_{i,j}^0\\&=\frac{1}{w_{i,j}^2}\left(\psi_{xx}+\psi_{yy}\right)_{i,j}+\left[\frac{\partial f(u)}{\partial t}\right]_{i,j}^0,\end{aligned} \tag{16}$$

$$\begin{aligned}\left(\frac{\partial^4 u}{\partial t^4}\right)_{i,j}^0&=\frac{\partial^2}{\partial t^2}\left(\frac{\partial^2 u}{\partial t^2}\right)_{i,j}^0\\&=\frac{\partial^2}{\partial t^2}\left[\frac{1}{w^2}\left(\frac{\partial^2 u}{\partial x^2}+\frac{\partial^2 u}{\partial y^2}\right)+f(u)\right]_{i,j}^0\\&=\frac{1}{w_{i,j}^2}\left[\left(\frac{\partial^2}{\partial x^2}+\frac{\partial^2}{\partial y^2}\right)\left(\frac{1}{w^2}\right)\left(\frac{\partial^2 u}{\partial x^2}+\frac{\partial^2 u}{\partial y^2}\right)\right]_{i,j}^0\\&\quad+2\frac{1}{w_{i,j}^2}\left\{\left[\frac{\partial}{\partial x}\left(\frac{1}{w^2}\right)\right]_{i,j}\left(\frac{\partial^3 u}{\partial x^3}+\frac{\partial^3 u}{\partial x\partial y^2}\right)_{i,j}^0+\left[\frac{\partial}{\partial y}\left(\frac{1}{w^2}\right)\right]_{i,j}\right.\\&\quad\left.\times\left(\frac{\partial^3 u}{\partial y^3}+\frac{\partial^3 u}{\partial y\partial x^2}\right)_{i,j}^0\right\}\\&\quad+\frac{1}{w_{i,j}^4}\left[2\left(\frac{\partial^4 u}{\partial x^2\partial y^2}\right)_{i,j}^0+\left(\frac{\partial^4 u}{\partial x^4}+\frac{\partial^4 u}{\partial y^4}\right)_{i,j}^0\right]\\&\quad+\frac{1}{w_{i,j}^2}\left[\frac{\partial^2 f(u)}{\partial x^2}+\frac{\partial^2 f(u)}{\partial y^2}\right]_{i,j}^0+\left[\frac{\partial^2 f(u)}{\partial t^2}\right]_{i,j}^0\\&=\frac{1}{w_{i,j}^2}\left\{\left[\left(\frac{1}{w^2}\right)_{xx}+\left(\frac{1}{w^2}\right)_{yy}\right]_{i,j}\left(\varphi_{xx}+\varphi_{yy}\right)_{i,j}\right.\\&\quad+2\left[\frac{\partial}{\partial x}\left(\frac{1}{w^2}\right)_{i,j}\right]\left(\varphi_{xxx}+\varphi_{xyy}\right)_{i,j}\\&\quad\left.+2\left[\frac{\partial}{\partial y}\left(\frac{1}{w^2}\right)_{i,j}\right]\left(\varphi_{yyy}+\varphi_{xxy}\right)_{i,j}\right\}\\&\quad+\frac{1}{w_{i,j}^4}\left(\varphi_{xxxx}+2\varphi_{xxyy}+\varphi_{yyyy}\right)_{i,j}\\&\quad+\frac{1}{w_{i,j}^2}\left[\frac{\partial^2 f(u)}{\partial x^2}+\frac{\partial^2 f(u)}{\partial y^2}\right]_{i,j}^0+\left[\frac{\partial^2 f(u)}{\partial t^2}\right]_{i,j}^0.\end{aligned} \tag{17}$$

Substituting Eqs. (15)-(17) into Eq. (13), and omitting $O\left(\tau^5\right)$, we have

$$\begin{aligned}u_{i,j}^{\frac{1}{2}}&=\varphi_{i,j}+\frac{\tau}{2}\psi_{i,j}+\frac{\tau^2}{8}\left[\frac{1}{w_{i,j}^2}\left(\varphi_{xx}+\varphi_{yy}\right)_{i,j}+f(u)_{i,j}^0\right]\\&\quad+\frac{\tau^3}{48}\left[\frac{1}{w_{i,j}^2}\left(\psi_{xx}+\psi_{yy}\right)_{i,j}\right]+\frac{\tau^4}{384}\left\{\frac{1}{w_{i,j}^2}\left[\left(\frac{1}{w^2}\right)_{xx}\right.\right.\\&\quad\left.+\left(\frac{1}{w^2}\right)_{yy}\right]_{i,j}\left(\varphi_{xx}+\varphi_{yy}\right)_{i,j}+\frac{1}{w_{i,j}^4}\left(\varphi_{xxxx}+\varphi_{yyyy}\right)_{i,j}\Big\}\\&\quad+\frac{\tau^4}{192}\left(\frac{1}{w_{i,j}^2}\right)\left\{\left[\left(\frac{1}{w^2}\right)_{x}\right]_{i,j}\left(\varphi_{xxx}+\varphi_{xyy}\right)_{i,j}\right.\\&\quad\left.+\left[\left(\frac{1}{w^2}\right)_{y}\right]_{i,j}\left(\varphi_{yyy}+\varphi_{xxy}\right)_{i,j}+\frac{1}{w_{i,j}^2}\left(\varphi_{xxyy}\right)_{i,j}\right\}\\&\quad+\frac{\tau^3}{48}\left[\frac{\partial f(u)}{\partial t}\right]_{i,j}^0+\frac{\tau^4}{384}\left\{\frac{1}{w_{i,j}^2}\left[\frac{\partial^2 f(u)}{\partial x^2}+\frac{\partial^2 f(u)}{\partial y^2}\right]_{i,j}^0\right.\\&\quad\left.+\left[\frac{\partial^2 f(u)}{\partial t^2}\right]_{i,j}^0\right\}.\end{aligned} \tag{18}$$

Similarly, substituting Eqs. (15)-(17) into Eq. (14), we have

$$\begin{aligned}u_{i,j}^1&=\varphi_{i,j}+\tau\psi_{i,j}+\frac{\tau^2}{2}\left[\frac{1}{w_{i,j}^2}\left(\varphi_{xx}+\varphi_{yy}\right)_{i,j}+f(u)_{i,j}^0\right]\\&\quad+\frac{\tau^3}{6}\left[\frac{1}{w_{i,j}^2}\left(\psi_{xx}+\psi_{yy}\right)_{i,j}\right]\\&\quad+\frac{\tau^4}{24}\left\{\frac{1}{w_{i,j}^2}\left[\left(\frac{1}{w^2}\right)_{xx}+\left(\frac{1}{w^2}\right)_{yy}\right]_{i,j}\left(\varphi_{xx}+\varphi_{yy}\right)_{i,j}\right.\end{aligned}$$

$$+\frac{1}{w_{i,j}^4}\left(\varphi_{xxxx}+\varphi_{yyyy}\right)_{i,j}\Bigg\}+\frac{\tau^4}{12}\left(\frac{1}{w_{i,j}^2}\right)$$
$$\times\Bigg\{\left[\left(\frac{1}{w^2}\right)_x\right]_{i,j}\left(\varphi_{xxx}+\varphi_{xyy}\right)_{i,j}$$
$$+\left[\left(\frac{1}{w^2}\right)_y\right]_{i,j}\left(\varphi_{yyy}+\varphi_{xxy}\right)_{i,j}+\frac{1}{w_{i,j}^2}\left(\varphi_{xxyy}\right)_{i,j}\Bigg\}$$
$$+\frac{\tau^3}{6}\left[\frac{\partial f(u)}{\partial t}\right]_{i,j}^0+\frac{\tau^4}{24}\Bigg\{\frac{1}{w_{i,j}^2}\left[\frac{\partial^2 f(u)}{\partial x^2}+\frac{\partial^2 f(u)}{\partial y^2}\right]_{i,j}^0$$
$$+\left[\frac{\partial^2 f(u)}{\partial t^2}\right]_{i,j}^0\Bigg\}. \tag{19}$$

2.3 Stability analysis

In this section, we consider the stability of the linear form of Eq. (1) i.e., $f\left(u_{i,j}^n\right)=f\left(x_i,y_j,t_n\right)$. At this time, Eqs. (10) and (12) are converted as follows

$$\left(\frac{5w_{i,j}^2}{3}+\frac{\lambda^2}{6}\right)u_{i,j}^{n+\frac{1}{2}}+\left(\frac{w_{i+1,j}^2}{6}-\frac{\lambda^2}{12}\right)u_{i+1,j}^{n+\frac{1}{2}}$$
$$+\left(\frac{w_{i-1,j}^2}{6}-\frac{\lambda^2}{12}\right)u_{i-1,j}^{n+\frac{1}{2}}=\left(\frac{10w_{i,j}^2}{3}-\frac{5\lambda^2}{3}\right)u_{i,j}^n \tag{20}$$
$$+\left(\frac{w_{i+1,j}^2}{3}+\frac{5\lambda^2}{6}\right)u_{i+1,j}^n+\left(\frac{w_{i-1,j}^2}{3}+\frac{5\lambda^2}{6}\right)u_{i-1,j}^n$$
$$-\left(\frac{5w_{i,j}^2}{3}+\frac{\lambda^2}{6}\right)u_{i,j}^{n-\frac{1}{2}}-\left(\frac{w_{i+1,j}^2}{6}-\frac{\lambda^2}{12}\right)u_{i+1,j}^{n-\frac{1}{2}}$$
$$-\left(\frac{w_{i-1,j}^2}{6}-\frac{\lambda^2}{12}\right)u_{i-1,j}^{n-\frac{1}{2}}+\frac{w_{i,j}^2\tau^2}{3}f_{i,j}^n+\frac{\tau^2}{24}$$
$$\times\left(w_{i+1,j}^2f_{i+1,j}^n+w_{i-1,j}^2f_{i-1,j}^n\right)+\frac{w_{i,j}^2\tau^2}{24}\left(f_{i,j}^{n+\frac{1}{2}}+f_{i,j}^{n-\frac{1}{2}}\right),$$
$$\left(\frac{5w_{i,j}^2}{3}+\frac{\lambda^2}{6}\right)u_{i,j}^{n+1}+\left(\frac{w_{i,j+1}^2}{6}-\frac{\lambda^2}{12}\right)u_{i,j+1}^{n+1}$$
$$+\left(\frac{w_{i,j-1}^2}{6}-\frac{\lambda^2}{12}\right)u_{i,j-1}^{n+1}=\left(\frac{10w_{i,j}^2}{3}-\frac{5\lambda^2}{3}\right)u_{i,j}^{n+\frac{1}{2}}$$
$$+\left(\frac{w_{i,j+1}^2}{3}+\frac{5\lambda^2}{6}\right)u_{i,j+1}^{n+\frac{1}{2}}+\left(\frac{w_{i,j-1}^2}{3}+\frac{5\lambda^2}{6}\right)u_{i,j-1}^{n+\frac{1}{2}}$$
$$-\left(\frac{5w_{i,j}^2}{3}+\frac{\lambda^2}{6}\right)u_{i,j}^{n}-\left(\frac{w_{i,j+1}^2}{6}-\frac{\lambda^2}{12}\right)u_{i,j+1}^{n}$$
$$-\left(\frac{w_{i,j-1}^2}{6}-\frac{\lambda^2}{12}\right)u_{i,j-1}^{n}+\frac{w_{i,j}^2\tau^2}{3}f_{i,j}^{n+\frac{1}{2}}+\frac{\tau^2}{24} \tag{21}$$
$$\times\left(w_{i,j+1}^2f_{i,j+1}^{n+\frac{1}{2}}+w_{i,j-1}^2f_{i,j-1}^{n+\frac{1}{2}}\right)+\frac{w_{i,j}^2\tau^2}{24}\left(f_{i,j}^{n+1}+f_{i,j}^n\right).$$

Theorem 1 *When*

$$\max_{1\le i,j\le N}\left|\frac{v_{i,j}\cdot\tau}{h}\right|=v_{\max}\lambda\le 0.8944, \tag{22}$$

the scheme is stable, in which, $v_{\max}=\max\limits_{1\le i,j\le N}|v_{i,j}|$.

Proof Letting $u_{i,j}^n=\eta^n e^{I\sigma_1x_i}e^{I\sigma_2y_j}$, $u_{i,j}^{n+\frac{1}{2}}=\eta^{n+\frac{1}{2}}e^{I\sigma_1x_i}e^{I\sigma_2y_j}$, $u_{i,j}^{n-\frac{1}{2}}=\eta^{n-\frac{1}{2}}e^{I\sigma_1x_i}e^{I\sigma_2y_j}$, where η^n, $\eta^{n+\frac{1}{2}}$ and $\eta^{n-\frac{1}{2}}$ are amplitudes. σ_1,σ_2 are wavenumber, and $I=\sqrt{-1}$ is the imaginary unit.

We assume that the function $f(x,y,t)$ is exact and no error. Omitting the function $f(x,y,t)$, letting $\max\limits_{1\le i,j\le N}v_{i,j}^2=a$, i.e., $\max\limits_{1\le i,j\le N}w_{i,j}^2=\frac{1}{a}$, and multiplying by a on the both sides of Eq. (20), we have

$$\left(\frac{5}{3}+\frac{a\lambda^2}{6}\right)\eta^{n+\frac{1}{2}}e^{I\sigma_1x_i}e^{I\sigma_2y_j}+\left(\frac{1}{6}-\frac{a\lambda^2}{12}\right)\eta^{n+\frac{1}{2}}$$
$$\times\left(e^{I\sigma_1x_{i+1}}e^{I\sigma_2y_j}+e^{I\sigma_1x_{i-1}}e^{I\sigma_2y_j}\right)=\left(\frac{10}{3}-\frac{5a\lambda^2}{3}\right)$$
$$\eta^n e^{I\sigma_1x_i}e^{I\sigma_2y_j}+\left(\frac{1}{3}+\frac{5a\lambda^2}{6}\right)\eta^n\Big(e^{I\sigma_1x_{i+1}}e^{I\sigma_2y_j}$$
$$+e^{I\sigma_1x_{i-1}}e^{I\sigma_2y_j}\Big)-\left(\frac{5}{3}+\frac{a\lambda^2}{6}\right)\eta^{n-\frac{1}{2}}e^{I\sigma_1x_i}e^{I\sigma_2y_j}$$
$$-\left(\frac{1}{6}-\frac{a\lambda^2}{12}\right)\eta^{n-\frac{1}{2}}\left(e^{I\sigma_1x_{i+1}}e^{I\sigma_2y_j}+e^{I\sigma_1x_{i-1}}e^{I\sigma_2y_j}\right). \tag{23}$$

By $e^{\pm I\sigma h}=\pm I\sin\sigma h+\cos\sigma h$, we get

$$\left(\frac{5}{3}+\frac{a\lambda^2}{6}\right)\eta^{n+\frac{1}{2}}+2\left(\frac{1}{6}-\frac{a\lambda^2}{12}\right)\eta^{n+\frac{1}{2}}\cos\sigma_1h$$
$$=\left(\frac{10}{3}-\frac{5a\lambda^2}{3}\right)\eta^n+2\left(\frac{1}{3}+\frac{5a\lambda^2}{6}\right)\eta^n\cos\sigma_1h$$
$$-\left(\frac{5}{3}+\frac{a\lambda^2}{6}\right)\eta^{n-\frac{1}{2}}-2\left(\frac{1}{6}-\frac{a\lambda^2}{12}\right)\eta^{n-\frac{1}{2}}\cos\sigma_1h. \tag{24}$$

Letting $\varepsilon^{n+\frac{1}{2}}=\eta^n$, $\varepsilon^n=\eta^{n-\frac{1}{2}}$, Eq. (24) is written in matrix form

$$\begin{bmatrix}\frac{5}{3}+\frac{a\lambda^2}{6}+2\left(\frac{1}{6}-\frac{a\lambda^2}{12}\right)\cos\sigma_1h & 0\\ 0 & 1\end{bmatrix}\begin{bmatrix}\eta^{n+\frac{1}{2}}\\ \varepsilon^{n+\frac{1}{2}}\end{bmatrix}=$$
$$\begin{bmatrix}\frac{10}{3}-\frac{5a\lambda^2}{3}+2\left(\frac{1}{3}+\frac{5a\lambda^2}{6}\right)\cos\sigma_1h & -\left(\frac{5}{3}+\frac{a\lambda^2}{6}\right)-2\left(\frac{1}{6}-\frac{a\lambda^2}{12}\right)\cos\sigma_1h\\ 1 & 0\end{bmatrix}$$
$$\times\begin{bmatrix}\eta^n\\ \varepsilon^n\end{bmatrix}. \tag{25}$$

Letting $U^n = (\eta^n, \varepsilon^n)^T$ and substituting it into Eq. (25) to get

$$\begin{bmatrix} \frac{5}{3}+\frac{a\lambda^2}{6}+2\left(\frac{1}{6}-\frac{a\lambda^2}{12}\right)\cos\sigma_1 h & 0 \\ 0 & 1 \end{bmatrix} U^{n+\frac{1}{2}} = \begin{bmatrix} \frac{10}{3}-\frac{5a\lambda^2}{3}+2\left(\frac{1}{3}+\frac{5a\lambda^2}{6}\right)\cos\sigma_1 h & -\left(\frac{5}{3}+\frac{a\lambda^2}{6}\right)-2\left(\frac{1}{6}-\frac{a\lambda^2}{12}\right)\cos\sigma_1 h \\ 1 & 0 \end{bmatrix} U^n. \tag{26}$$

Similarly, Eq. (21) can be treated as

$$\begin{bmatrix} \frac{5}{3}+\frac{a\lambda^2}{6}+2\left(\frac{1}{6}-\frac{a\lambda^2}{12}\right)\cos\sigma_2 h & 0 \\ 0 & 1 \end{bmatrix} U^{n+1} = \begin{bmatrix} \frac{10}{3}-\frac{5a\lambda^2}{3}+2\left(\frac{1}{3}+\frac{5a\lambda^2}{6}\right)\cos\sigma_2 h & -\left(\frac{5}{3}+\frac{a\lambda^2}{6}\right)-2\left(\frac{1}{6}-\frac{a\lambda^2}{12}\right)\cos\sigma_2 h \\ 1 & 0 \end{bmatrix} \times U^{n+\frac{1}{2}}. \tag{27}$$

Substituting Eq. (26) into Eq. (27), the error propagation matrix is

$$G = \begin{bmatrix} \frac{BD}{AC}-1 & -\frac{B}{A} \\ \frac{D}{C} & -1 \end{bmatrix},$$

in which,

$$\begin{aligned} A &= \frac{5}{3}+\frac{a\lambda^2}{6}+2\left(\frac{1}{6}-\frac{a\lambda^2}{12}\right)\cos\sigma_1 h, \\ B &= \frac{10}{3}-\frac{5a\lambda^2}{3}+2\left(\frac{1}{3}+\frac{5a\lambda^2}{6}\right)\cos\sigma_1 h, \\ C &= \frac{5}{3}+\frac{a\lambda^2}{6}+2\left(\frac{1}{6}-\frac{a\lambda^2}{12}\right)\cos\sigma_2 h, \\ D &= \frac{10}{3}-\frac{5a\lambda^2}{3}+2\left(\frac{1}{3}+\frac{5a\lambda^2}{6}\right)\cos\sigma_2 h. \end{aligned}$$

The characteristic equation can be obtained by

$$|\mu I - G| = \mu^2 - \left(\frac{BD}{AC}-2\right)\mu + 1 = 0.$$

From the Lemma 1 in Appendix A, we know that when $|b_1| = |\frac{BD}{AC}-2| \le 2$, i.e., $0 \le \frac{BD}{AC} \le 4$, the scheme is stable. Here,

$$\frac{BD}{AC} = \frac{\left[\frac{10}{3}-\frac{5a\lambda^2}{3}+2\left(\frac{1}{3}+\frac{5a\lambda^2}{6}\right)\cos\sigma_1 h\right]\cdot\left[\frac{10}{3}-\frac{5a\lambda^2}{3}+2\left(\frac{1}{3}+\frac{5a\lambda^2}{6}\right)\cos\sigma_2 h\right]}{\left[\frac{5}{3}+\frac{a\lambda^2}{6}+2\left(\frac{1}{6}-\frac{a\lambda^2}{12}\right)\cos\sigma_1 h\right]\cdot\left[\frac{5}{3}+\frac{a\lambda^2}{6}+2\left(\frac{1}{6}-\frac{a\lambda^2}{12}\right)\cos\sigma_2 h\right]},$$

in which,

$$\begin{aligned} A &= \left[\frac{5}{3}+\frac{a\lambda^2}{6}+2\left(\frac{1}{6}-\frac{a\lambda^2}{12}\right)\cos\sigma_1 h\right] = \frac{5}{3}+\frac{1}{3}\cos\sigma_1 h \\ &\quad + (1-\cos\sigma_1 h)\frac{a\lambda^2}{6} > 0, \\ C &= \left[\frac{5}{3}+\frac{a\lambda^2}{6}+2\left(\frac{1}{6}-\frac{a\lambda^2}{12}\right)\cos\sigma_2 h\right] = \frac{5}{3}+\frac{1}{3}\cos\sigma_2 h \\ &\quad + (1-\cos\sigma_2 h)\frac{a\lambda^2}{6} > 0. \end{aligned}$$

Firstly, we solve the inequality $\frac{BD}{AC} \le 4$, i.e., $BD \le 4AC$,

$$\begin{aligned} &\frac{100+25a^2\lambda^4-100a\lambda^2}{9}+\frac{20-25a^2\lambda^4+40a\lambda^2}{9} \\ &(\cos\sigma_1 h+\cos\sigma_2 h)+\frac{4+25a^2\lambda^4+20a\lambda^2}{9}\cos\sigma_1 h\cos\sigma_2 h \\ &\le \frac{100+a^2\lambda^4+20a\lambda^2}{9}+\frac{20-a^2\lambda^4-8a\lambda^2}{9} \\ &\quad (\cos\sigma_1 h+\cos\sigma_2 h)+\frac{4+a^2\lambda^4-4a\lambda^2}{9}\cos\sigma_1 h\cos\sigma_2 h. \end{aligned}$$

We get

$$\begin{aligned} &a\lambda^2-5+\left(2-a\lambda^2\right)(\cos\sigma_1 h+\cos\sigma_2 h) \\ &+\left(1+a\lambda^2\right)\cos\sigma_1 h\cos\sigma_2 h \le 0, \end{aligned} \tag{28}$$

Due to

$$\cos\sigma_1 h+\cos\sigma_2 h = 2\cos\frac{\sigma_1 h+\sigma_2 h}{2}\cos\frac{\sigma_1 h-\sigma_2 h}{2}.$$

Inequality(28) can be expressed as

$$\begin{aligned} &a\lambda^2\left(1-2\cos\tfrac{\sigma_1 h+\sigma_2 h}{2}\cos\tfrac{\sigma_1 h-\sigma_2 h}{2}+\cos\sigma_1 h\cos\sigma_2 h\right) \\ &\le 5-4\cos\tfrac{\sigma_1 h+\sigma_2 h}{2}\cos\tfrac{\sigma_1 h-\sigma_2 h}{2}-\cos\sigma_1 h\cos\sigma_2 h. \end{aligned} \tag{29}$$

When $\left(1-2\cos\frac{\sigma_1 h+\sigma_2 h}{2}\cos\frac{\sigma_1 h-\sigma_2 h}{2}+\cos\sigma_1 h\cos\sigma_2 h\right) \le 0$, inequality (29) always holds.
When $\left(1-2\cos\frac{\sigma_1 h+\sigma_2 h}{2}\cos\frac{\sigma_1 h-\sigma_2 h}{2}+\cos\sigma_1 h\cos\sigma_2 h\right) > 0$, only need to make

$$a\lambda^2 \le 2+\frac{3-3\cos\sigma_1 h\cos\sigma_2 h}{1-2\cos\frac{\sigma_1 h+\sigma_2 h}{2}\cos\frac{\sigma_1 h-\sigma_2 h}{2}+\cos\sigma_1 h\cos\sigma_2 h}.$$

At this time,

$$a\lambda^2 \le 2.$$

Then, we solve the inequality $0 \leq \frac{BD}{AC}$, i.e., $BD \geq 0$

$$\left[\frac{10}{3}-\frac{5a\lambda^2}{3}+2\left(\frac{1}{3}+\frac{5a\lambda^2}{6}\right)\cos\sigma_1 h\right]\cdot \left[\frac{10}{3}-\frac{5a\lambda^2}{3}+2\left(\frac{1}{3}+\frac{5a\lambda^2}{6}\right)\cos\sigma_2 h\right]\geq 0. \tag{30}$$

Letting $\cos\sigma h = \theta$ and $F(\theta) = \frac{10}{3} - \frac{5a\lambda^2}{3} + 2\left(\frac{1}{3}+\frac{5a\lambda^2}{6}\right)\theta$, $\theta \in [-1,1]$, $F'(\theta) = 2\left(\frac{1}{3}+\frac{5a\lambda^2}{6}\right) \geq 0$. So $F(\theta)$ is an increasing function. Due to $F_{\min} = F(-1) = \frac{8}{3} - \frac{10a\lambda^2}{3}$ and $F_{\max} = F(1) = 4$, therefore, when $F(-1) = \frac{8}{3} - \frac{10a\lambda^2}{3} \geq 0$, i.e., $a\lambda^2 \leq \frac{4}{5}$, the inequality (30) holds.

In summary, when $v_{\max}\lambda = \sqrt{a}\lambda \leq 0.8944$, the scheme is stable. □

3 Extend to the 3D case

We consider the 3D nonlinear wave equation with variable wave velocity as follows

$$\frac{\partial^2 u}{\partial t^2} = v^2(x,y,z)\left(\frac{\partial^2 u}{\partial x^2}+\frac{\partial^2 u}{\partial y^2}+\frac{\partial^2 u}{\partial z^2}\right) + f(u), (x,y,z,t) \in \Omega \times (0,T], \tag{31}$$

with the initial conditions

$$\begin{aligned} u(x,y,z,0) &= \varphi(x,y,z), \\ \frac{\partial u(x,y,z,0)}{\partial t} &= \psi(x,y,z), \quad (x,y,z) \in \Omega, \end{aligned} \tag{32}$$

and the Dirichlet boundary condition

$$u(x,y,z,t) = g(x,y,z,t), \quad (x,y,z,t) \in \partial\Omega \times (0,T], \tag{33}$$

where $\Omega \in (d_1, d_2)^3$, other definitions are similar to the 2D problem. The grid points are denoted as (x_i, y_j, z_k, t_n), in which, $x_i = d_1 + ih$, $y_j = d_1 + jh$, $z_k = d_1 + kh$, $t_n = n\tau$, $i, j, k = 0, 1, \cdots, N$, $n = 0, 1, \cdots, M$.

Letting $w^2(x,y,z) = \frac{1}{v^2(x,y,z)}$, the LOD technique [35] is applied to split the 3D problem (31) as follows

$$\frac{1}{3}w^2(x,y,z)\frac{\partial^2 u}{\partial t^2} = \frac{\partial^2 u}{\partial x^2} + \frac{1}{3}w^2(x,y,z) f(u), \tag{34}$$

$$\frac{1}{3}w^2(x,y,z)\frac{\partial^2 u}{\partial t^2} = \frac{\partial^2 u}{\partial y^2} + \frac{1}{3}w^2(x,y,z) f(u), \tag{35}$$

$$\frac{1}{3}w^2(x,y,z)\frac{\partial^2 u}{\partial t^2} = \frac{\partial^2 u}{\partial z^2} + \frac{1}{3}w^2(x,y,z) f(u). \tag{36}$$

3.1 Implicit compact difference scheme

Firstly, we consider Eq. (34) at grid point (x_i, y_j, z_k, t_n), i.e.,

$$\frac{1}{3}w^2_{i,j,k}\left(\frac{\partial^2 u}{\partial t^2}\right)^n_{i,j,k} = \left(\frac{\partial^2 u}{\partial x^2}\right)^n_{i,j,k} + \frac{1}{3}w^2_{i,j,k} f(u^n_{i,j,k}). \tag{37}$$

In Eq. (37), the $\frac{\partial^2 u}{\partial t^2}$ and $\frac{\partial^2 u}{\partial x^2}$ are discretized by the fourth-order compact difference method [34]

$$\begin{aligned} &\frac{1}{3}w^2_{i,j,k}\left(1+\frac{(\tau/3)^2}{12}\delta_t^2\right)^{-1}\delta_t^2 u^n_{i,j,k} \\ &= \left(1+\frac{h^2}{12}\delta_x^2\right)^{-1}\delta_x^2 u^n_{i,j,k} + \frac{1}{3}w^2_{i,j,k} f(u^n_{i,j,k}) + O\left(\tau^4+h^4\right), \end{aligned} \tag{38}$$

in which,

$$\delta_x^2 u^n_{i,j,k} = \frac{u^n_{i+1,j,k} - 2u^n_{i,j,k} + u^n_{i-1,j,k}}{h^2},$$

$$\delta_t^2 u^n_{i,j,k} = \frac{u^{n+\frac{1}{3}}_{i,j,k} - 2u^n_{i,j,k} + u^{n-\frac{1}{3}}_{i,j,k}}{(\tau/3)^2}.$$

Noticing that the high-order term $\left(\frac{h^2}{12}\delta_x^2 \cdot \frac{(\tau/3)^2}{12}\delta_t^2\right) w^2_{i,j,k} f(u^n_{i,j,k})$ as a high-order truncation error term, i.e., $O\left(\tau^2 h^2\right)$, Eq. (38) can be rewritten as

$$\begin{aligned} &\left(1+\frac{h^2}{12}\delta_x^2\right) w^2_{i,j,k}\left[\frac{u^{n+\frac{1}{3}}_{i,j,k} - 2u^n_{i,j,k} + u^{n-\frac{1}{3}}_{i,j,k}}{(\tau/3)^2}\right] \\ &= 3\delta_x^2\left(\frac{1}{12}u^{n+\frac{1}{3}}_{i,j,k} + \frac{5}{6}u^n_{i,j,k} + \frac{1}{12}u^{n-\frac{1}{3}}_{i,j,k}\right) \\ &\quad + \frac{2w^2_{i,j,k}}{3} f(u^n_{i,j,k}) + \frac{1}{12}\left[w^2_{i+1,j,k} f(u^n_{i+1,j,k})\right. \\ &\quad \left. + w^2_{i-1,j,k} f(u^n_{i-1,j,k})\right] + \frac{w^2_{i,j,k}}{12}\left[f(u^{n+\frac{1}{3}}_{i,j,k}) + f(u^{n-\frac{1}{3}}_{i,j,k})\right] \\ &\quad + O\left(\tau^4 + \tau^2 h^2 + h^4\right). \end{aligned} \tag{39}$$

Multiplying both sides of Eq. (39) by $\frac{\tau^2}{9}$ and omitting the truncation error term, i.e.,

$$\begin{aligned} &\left(\frac{5w^2_{i,j,k}}{6} + \frac{\lambda^2}{18}\right) u^{n+\frac{1}{3}}_{i,j,k} + \left(\frac{w^2_{i+1,j,k}}{12} - \frac{\lambda^2}{36}\right) u^{n+\frac{1}{3}}_{i+1,j,k} \\ &+ \left(\frac{w^2_{i-1,j,k}}{12} - \frac{\lambda^2}{36}\right) u^{n+\frac{1}{3}}_{i-1,j,k} = \left(\frac{5w^2_{i,j,k}}{3} - \frac{5\lambda^2}{9}\right) u^n_{i,j,k} \end{aligned}$$

$$+\left(\frac{w_{i+1,j,k}^2}{6}+\frac{5\lambda^2}{18}\right)u_{i+1,j,k}^{n}+\left(\frac{w_{i-1,j,k}^2}{6}+\frac{5\lambda^2}{18}\right)u_{i-1,j,k}^{n}$$
$$-\left(\frac{5w_{i,j,k}^2}{6}+\frac{\lambda^2}{18}\right)u_{i,j,k}^{n-\frac{1}{3}}-\left(\frac{w_{i+1,j,k}^2}{12}-\frac{\lambda^2}{36}\right)u_{i+1,j,k}^{n-\frac{1}{3}}$$
$$-\left(\frac{w_{i-1,j,k}^2}{12}-\frac{\lambda^2}{36}\right)u_{i-1,j,k}^{n-\frac{1}{3}}+\frac{2w_{i,j,k}^2\tau^2}{27}f(u_{i,j,k}^{n})$$
$$+\frac{\tau^2}{108}\left[w_{i+1,j,k}^2 f(u_{i+1,j,k}^{n})+w_{i-1,j,k}^2 f(u_{i-1,j,k}^{n})\right]$$
$$+\frac{w_{i,j,k}^2\tau^2}{108}\left[f(u_{i,j,k}^{n+\frac{1}{3}})+f(u_{i,j,k}^{n-\frac{1}{3}})\right]. \tag{40}$$

Secondly, we consider Eq. (35) at the grid point $\left(x_i, y_j, z_k, t_{n+\frac{1}{3}}\right)$, i.e.,

$$\frac{1}{3}w_{i,j,k}^2\left(\frac{\partial^2 u}{\partial t^2}\right)_{i,j,k}^{n+\frac{1}{3}}=\left(\frac{\partial^2 u}{\partial y^2}\right)_{i,j,k}^{n+\frac{1}{3}}+\frac{1}{3}w_{i,j,k}^2 f(u_{i,j,k}^{n+\frac{1}{3}}). \tag{41}$$

Using similar method, we obtain

$$\left(\frac{5w_{i,j,k}^2}{6}+\frac{\lambda^2}{18}\right)u_{i,j,k}^{n+\frac{2}{3}}+\left(\frac{w_{i,j+1,k}^2}{12}-\frac{\lambda^2}{36}\right)u_{i,j+1,k}^{n+\frac{2}{3}}$$
$$+\left(\frac{w_{i,j-1,k}^2}{12}-\frac{\lambda^2}{36}\right)u_{i,j-1,k}^{n+\frac{2}{3}}=\left(\frac{5w_{i,j,k}^2}{3}-\frac{5\lambda^2}{9}\right)u_{i,j,k}^{n+\frac{1}{3}}$$
$$+\left(\frac{w_{i,j+1,k}^2}{6}+\frac{5\lambda^2}{18}\right)u_{i,j+1,k}^{n+\frac{1}{3}}+\left(\frac{w_{i,j-1,k}^2}{6}+\frac{5\lambda^2}{18}\right)u_{i,j-1,k}^{n+\frac{1}{3}}$$
$$-\left(\frac{5w_{i,j,k}^2}{6}+\frac{\lambda^2}{18}\right)u_{i,j,k}^{n}-\left(\frac{w_{i,j+1,k}^2}{12}-\frac{\lambda^2}{36}\right)u_{i,j+1,k}^{n}$$
$$-\left(\frac{w_{i,j-1,k}^2}{12}-\frac{\lambda^2}{36}\right)u_{i,j-1,k}^{n}+\frac{2w_{i,j,k}^2\tau^2}{27}f(u_{i,j,k}^{n+\frac{1}{3}})$$
$$+\frac{\tau^2}{108}\left[w_{i,j+1,k}^2 f(u_{i,j+1,k}^{n+\frac{1}{3}})+w_{i,j-1,k}^2 f(u_{i,j-1,k}^{n+\frac{1}{3}})\right]$$
$$+\frac{w_{i,j,k}^2\tau^2}{108}\left[f(u_{i,j,k}^{n+\frac{2}{3}})+f(u_{i,j,k}^{n})\right]. \tag{42}$$

Finally, we consider Eq. (36) at the grid point $\left(x_i, y_j, z_k, t_{n+\frac{2}{3}}\right)$, i.e.,

$$\frac{1}{3}w_{i,j,k}^2\left(\frac{\partial^2 u}{\partial t^2}\right)_{i,j,k}^{n+\frac{2}{3}}=\left(\frac{\partial^2 u}{\partial z^2}\right)_{i,j,k}^{n+\frac{2}{3}}+\frac{1}{3}w_{i,j,k}^2 f(u_{i,j,k}^{n+\frac{2}{3}}). \tag{43}$$

Using similar method, we obtain

$$\left(\frac{5w_{i,j,k}^2}{6}+\frac{\lambda^2}{18}\right)u_{i,j,k}^{n+1}+\left(\frac{w_{i,j,k+1}^2}{12}-\frac{\lambda^2}{36}\right)u_{i,j,k+1}^{n+1}$$
$$+\left(\frac{w_{i,j,k-1}^2}{12}-\frac{\lambda^2}{36}\right)u_{i,j,k-1}^{n+1}=\left(\frac{5w_{i,j,k}^2}{3}-\frac{5\lambda^2}{9}\right)u_{i,j,k}^{n+\frac{2}{3}}$$
$$+\left(\frac{w_{i,j,k+1}^2}{6}+\frac{5\lambda^2}{18}\right)u_{i,j,k+1}^{n+\frac{2}{3}}+\left(\frac{w_{i,j,k-1}^2}{6}+\frac{5\lambda^2}{18}\right)u_{i,j,k-1}^{n+\frac{2}{3}}$$
$$-\left(\frac{5w_{i,j,k}^2}{6}+\frac{\lambda^2}{18}\right)u_{i,j,k}^{n+\frac{1}{3}}-\left(\frac{w_{i,j,k+1}^2}{12}-\frac{\lambda^2}{36}\right)u_{i,j,k+1}^{n+\frac{1}{3}}$$
$$-\left(\frac{w_{i,j,k-1}^2}{12}-\frac{\lambda^2}{36}\right)u_{i,j,k-1}^{n+\frac{1}{3}}+\frac{2w_{i,j,k}^2\tau^2}{27}f(u_{i,j,k}^{n+\frac{2}{3}})$$
$$+\frac{\tau^2}{108}\left[w_{i,j,k+1}^2 f(u_{i,j,k+1}^{n+\frac{2}{3}})+w_{i,j,k-1}^2 f(u_{i,j,k-1}^{n+\frac{2}{3}})\right]$$
$$+\frac{w_{i,j,k}^2\tau^2}{108}\left[f(u_{i,j,k}^{n+1})+f(u_{i,j,k}^{n+\frac{1}{3}})\right]. \tag{44}$$

According to the derivation process, Eqs. (40), (42) and (44) can be used to solve Eq. (31). As the HOC-LOD scheme for solving the 3D problem is a five-step scheme, it requires to compute the values of $u_{i,j,k}^{\frac{2}{3}}$ and $u_{i,j,k}^{1}$ in advance. Using the similar derivation process for the 2D case, we can get

$$u_{i,j,k}^{\frac{2}{3}}=\varphi_{i,j,k}+\frac{2\tau}{3}\psi_{i,j,k}+\frac{2\tau^2}{9}\left(\frac{1}{w_{i,j,k}^2}\right)\left(\varphi_{xx}+\varphi_{yy}\right.$$
$$\left.+\varphi_{zz}\right)_{i,j,k}+\frac{4\tau^3}{81}\left(\frac{1}{w_{i,j,k}^2}\right)\left(\psi_{xx}+\psi_{yy}+\psi_{zz}\right)_{i,j,k}$$
$$+\frac{2\tau^4}{243}\left[\frac{1}{w_{i,j,k}^4}\left(\varphi_{xxxx}+\varphi_{yyyy}+\varphi_{zzzz}+2\varphi_{xxyy}\right.\right.$$
$$\left.\left.+2\varphi_{xxzz}+2\varphi_{yyzz}\right)_{i,j,k}\right]+\frac{2\tau^4}{243}\left(\frac{1}{w_{i,j,k}^2}\right)$$
$$\left\{\left[\left(\frac{1}{w^2}\right)_{xx}+\left(\frac{1}{w^2}\right)_{yy}+\left(\frac{1}{w^2}\right)_{zz}\right]_{i,j,k}\right.$$
$$\left(\varphi_{xx}+\varphi_{yy}+\varphi_{zz}\right)_{i,j,k}+2\left[\left(\frac{1}{w^2}\right)_{x}\right]_{i,j,k}$$
$$\left(\varphi_{xxx}+\varphi_{xyy}+\varphi_{xzz}\right)_{i,j,k}+2\left[\left(\frac{1}{w^2}\right)_{y}\right]_{i,j,k}$$
$$\left(\varphi_{yyy}+\varphi_{xxy}+\varphi_{yzz}\right)_{i,j,k}$$
$$\left.+2\left[\left(\frac{1}{w^2}\right)_{z}\right]_{i,j,k}\left(\varphi_{zzz}+\varphi_{xxz}+\varphi_{yyz}\right)_{i,j,k}\right\}$$
$$+\frac{2\tau^2}{9}f(u)_{i,j,k}^{0}+\frac{4\tau^3}{81}\left[\frac{\partial f(u)}{\partial t}\right]_{i,j,k}^{0}$$

$$+\frac{2\tau^4}{243}\left\{\frac{1}{w_{i,j,k}^2}\left[\frac{\partial^2 f(u)}{\partial x^2}+\frac{\partial^2 f(u)}{\partial y^2}+\frac{\partial^2 f(u)}{\partial z^2}\right]_{i,j,k}^{0}+\left[\frac{\partial^2 f(u)}{\partial t^2}\right]_{i,j,k}^{0}\right\},$$

and

$$\begin{aligned}u_{i,j,k}^{1}=&\varphi_{i,j,k}+\tau\psi_{i,j,k}+\frac{\tau^2}{2}\left(\frac{1}{w_{i,j,k}^2}\right)\left(\varphi_{xx}+\varphi_{yy}+\varphi_{zz}\right)_{i,j,k}\\&+\frac{\tau^3}{6}\left(\frac{1}{w_{i,j,k}^2}\right)\left(\psi_{xx}+\psi_{yy}+\psi_{zz}\right)_{i,j,k}\\&+\frac{\tau^4}{24}\left[\frac{1}{w_{i,j,k}^4}\left(\varphi_{xxxx}+\varphi_{yyyy}+\varphi_{zzzz}+2\varphi_{xxyy}\right.\right.\\&\left.\left.+2\varphi_{xxzz}+2\varphi_{yyzz}\right)_{i,j,k}\right]+\frac{\tau^4}{24}\left(\frac{1}{w_{i,j,k}^2}\right)\\&\left\{\left[\left(\frac{1}{w^2}\right)_{xx}+\left(\frac{1}{w^2}\right)_{yy}+\left(\frac{1}{w^2}\right)_{zz}\right]_{i,j,k}\right.\\&\left(\varphi_{xx}+\varphi_{yy}+\varphi_{zz}\right)_{i,j,k}+2\left[\left(\frac{1}{w^2}\right)_{x}\right]_{i,j,k}\\&\left(\varphi_{xxx}+\varphi_{xyy}+\varphi_{xzz}\right)_{i,j,k}+2\left[\left(\frac{1}{w^2}\right)_{y}\right]_{i,j,k}\\&\left(\varphi_{yyy}+\varphi_{xxy}+\varphi_{yzz}\right)_{i,j,k}\\&\left.2\left[\left(\frac{1}{w^2}\right)_{z}\right]_{i,j,k}\left(\varphi_{zzz}+\varphi_{xxz}+\varphi_{yyz}\right)_{i,j,k}\right\}\\&+\frac{\tau^2}{2}f(u)_{i,j,k}^{0}+\frac{\tau^3}{6}\left[\frac{\partial f(u)}{\partial t}\right]_{i,j,k}^{0}\\&+\frac{\tau^4}{24}\left\{\frac{1}{w_{i,j,k}^2}\left[\frac{\partial^2 f(u)}{\partial x^2}+\frac{\partial^2 f(u)}{\partial y^2}+\frac{\partial^2 f(u)}{\partial z^2}\right]_{i,j,k}^{0}\right.\\&\left.+\left[\frac{\partial^2 f(u)}{\partial t^2}\right]_{i,j,k}^{0}\right\}.\end{aligned}$$

3.2 Stability analysis

Similarly, we consider the stability of the linear form of Eq. (31) i.e., $f\left(u_{i,j,k}^{n}\right)=f\left(x_i,y_j,z_k,t_n\right)$. At this time, Eqs. (40), (42) and (44) are converted as follows

$$\begin{aligned}&\left(\frac{5w_{i,j,k}^2}{6}+\frac{\lambda^2}{18}\right)u_{i,j,k}^{n+\frac{1}{3}}+\left(\frac{w_{i+1,j,k}^2}{12}-\frac{\lambda^2}{36}\right)u_{i+1,j,k}^{n+\frac{1}{3}}\\&+\left(\frac{w_{i-1,j,k}^2}{12}-\frac{\lambda^2}{36}\right)u_{i-1,j,k}^{n+\frac{1}{3}}=\left(\frac{5w_{i,j,k}^2}{3}-\frac{5\lambda^2}{9}\right)u_{i,j,k}^{n}\\&+\left(\frac{w_{i+1,j,k}^2}{6}+\frac{5\lambda^2}{18}\right)u_{i+1,j,k}^{n}+\left(\frac{w_{i-1,j,k}^2}{6}+\frac{5\lambda^2}{18}\right)u_{i-1,j,k}^{n}\\&-\left(\frac{5w_{i,j,k}^2}{6}+\frac{\lambda^2}{18}\right)u_{i,j,k}^{n-\frac{1}{3}}-\left(\frac{w_{i+1,j,k}^2}{12}-\frac{\lambda^2}{36}\right)u_{i+1,j,k}^{n-\frac{1}{3}}\\&-\left(\frac{w_{i-1,j,k}^2}{12}-\frac{\lambda^2}{36}\right)u_{i-1,j,k}^{n-\frac{1}{3}}+\frac{2w_{i,j,k}^2\tau^2}{27}f_{i,j,k}^{n}\\&+\frac{\tau^2}{108}\left(w_{i+1,j,k}^2f_{i+1,j,k}^{n}+w_{i-1,j,k}^2f_{i-1,j,k}^{n}\right)\\&+\frac{w_{i,j,k}^2\tau^2}{108}\left(f_{i,j,k}^{n+\frac{1}{3}}+f_{i,j,k}^{n-\frac{1}{3}}\right),\end{aligned}\tag{45}$$

$$\begin{aligned}&\left(\frac{5w_{i,j,k}^2}{6}+\frac{\lambda^2}{18}\right)u_{i,j,k}^{n+\frac{2}{3}}+\left(\frac{w_{i,j+1,k}^2}{12}-\frac{\lambda^2}{36}\right)u_{i,j+1,k}^{n+\frac{2}{3}}\\&+\left(\frac{w_{i,j-1,k}^2}{12}-\frac{\lambda^2}{36}\right)u_{i,j-1,k}^{n+\frac{2}{3}}=\left(\frac{5w_{i,j,k}^2}{3}-\frac{5\lambda^2}{9}\right)u_{i,j,k}^{n+\frac{1}{3}}\\&+\left(\frac{w_{i,j+1,k}^2}{6}+\frac{5\lambda^2}{18}\right)u_{i,j+1,k}^{n+\frac{1}{3}}+\left(\frac{w_{i,j-1,k}^2}{6}+\frac{5\lambda^2}{18}\right)u_{i,j-1,k}^{n+\frac{1}{3}}\\&-\left(\frac{5w_{i,j,k}^2}{6}+\frac{\lambda^2}{18}\right)u_{i,j,k}^{n}-\left(\frac{w_{i,j+1,k}^2}{12}-\frac{\lambda^2}{36}\right)u_{i,j+1,k}^{n}\\&-\left(\frac{w_{i,j-1,k}^2}{12}-\frac{\lambda^2}{36}\right)u_{i,j-1,k}^{n}+\frac{2w_{i,j,k}^2\tau^2}{27}f_{i,j,k}^{n+\frac{1}{3}}\\&+\frac{\tau^2}{108}\left(w_{i,j+1,k}^2f_{i,j+1,k}^{n+\frac{1}{3}}+w_{i,j-1,k}^2f_{i,j-1,k}^{n+\frac{1}{3}}\right)\\&+\frac{w_{i,j,k}^2\tau^2}{108}\left(f_{i,j,k}^{n+\frac{2}{3}}+f_{i,j,k}^{n}\right),\end{aligned}\tag{46}$$

$$\begin{aligned}&\left(\frac{5w_{i,j,k}^2}{6}+\frac{\lambda^2}{18}\right)u_{i,j,k}^{n+1}+\left(\frac{w_{i,j,k+1}^2}{12}-\frac{\lambda^2}{36}\right)u_{i,j,k+1}^{n+1}\\&+\left(\frac{w_{i,j,k-1}^2}{12}-\frac{\lambda^2}{36}\right)u_{i,j,k-1}^{n+1}=\left(\frac{5w_{i,j,k}^2}{3}-\frac{5\lambda^2}{9}\right)u_{i,j,k}^{n+\frac{2}{3}}\\&+\left(\frac{w_{i,j,k+1}^2}{6}+\frac{5\lambda^2}{18}\right)u_{i,j,k+1}^{n+\frac{2}{3}}+\left(\frac{w_{i,j,k-1}^2}{6}+\frac{5\lambda^2}{18}\right)u_{i,j,k-1}^{n+\frac{2}{3}}\\&-\left(\frac{5w_{i,j,k}^2}{6}+\frac{\lambda^2}{18}\right)u_{i,j,k}^{n+\frac{1}{3}}-\left(\frac{w_{i,j,k+1}^2}{12}-\frac{\lambda^2}{36}\right)u_{i,j,k+1}^{n+\frac{1}{3}}\\&-\left(\frac{w_{i,j,k-1}^2}{12}-\frac{\lambda^2}{36}\right)u_{i,j,k-1}^{n+\frac{1}{3}}+\frac{2w_{i,j,k}^2\tau^2}{27}f_{i,j,k}^{n+\frac{2}{3}}\\&+\frac{\tau^2}{108}\left(w_{i,j,k+1}^2f_{i,j,k+1}^{n+\frac{2}{3}}+w_{i,j,k-1}^2f_{i,j,k-1}^{n+\frac{2}{3}}\right)\\&+\frac{w_{i,j,k}^2\tau^2}{108}\left(f_{i,j,k}^{n+1}+f_{i,j,k}^{n+\frac{1}{3}}\right).\end{aligned}\tag{47}$$

Similar to the derivation of Theorem 1, we can get that the above scheme is stable if

$$\max_{1\le i,j,k\le N}|\frac{v_{i,j,k}\cdot\tau}{h}| = v_{\max}\lambda \le 0.7385,$$

in which, $v_{\max} = \max_{1\le i,j,k\le N}|v_{i,j,k}|$. See Theorem 2 in Appendix A for detailed proof.

4 Numerical experiments

In this section, some numerical examples with the Dirichlet boundary conditions are conducted to illustrate the accuracy and effectiveness of these two HOC-LOD schemes. These programs are coded in Fortran 90 and executed on a laptop computer with an Intel Core i5-4210U CPU@1.70GHz 2.40GHz and 4GB of RAM.

$\|e_h\|_2$ and $\|e_h\|_\infty$ are defined as follows

$$\|e_h\|_\infty = \max_{0\le i,j\le N}|u^M_{i,j} - u\left(x_i, y_j, t_M\right)| \ \ or$$
$$\|e_h\|_\infty = \max_{0\le i,j,k\le N}|u^M_{i,j,k} - u\left(x_i, y_j, z_k, t_M\right)|,$$

$$\|e_h\|_2 = \sqrt{h^2\sum_{i,j=0}^{N}\left[u^M_{i,j} - u\left(x_i, y_j, t_M\right)\right]^2} \ \ or$$
$$\|e_h\|_2 = \sqrt{h^3\sum_{i,j,k=0}^{N}\left[u^M_{i,j,k} - u\left(x_i, y_j, z_k, t_M\right)\right]^2}.$$

The convergence order can be computed as follows

$$Order = \frac{\log\left(\|e_{h_1}\|_\infty/\|e_{h_2}\|_\infty\right)}{\log\left(h_1/h_2\right)} \ \ or$$
$$Order = \frac{\log\left(\|e_{h_1}\|_2/\|e_{h_2}\|_2\right)}{\log\left(h_1/h_2\right)}.$$

Table 1 The $\|e_h\|_\infty$ and $Order$ at $T = 1$ with various h and τ for Problem 1

(h, τ)	NCV-CPD-ADI [6]		HOC-LOD	
	$\|e_h\|_\infty$	$Order$	$\|e_h\|_\infty$	$Order$
$(\pi/40, 1/80)$	2.7242(-6)		2.5511(-8)	
$(\pi/80, 1/160)$	2.2523(-7)	3.5964	1.5702(-9)	4.0221
$(\pi/160, 1/320)$	1.7543(-8)	3.6824	9.6744(-11)	4.0206
$(\pi/320, 1/640)$	1.2928(-9)	3.7623	7.7555(-12)	3.6409

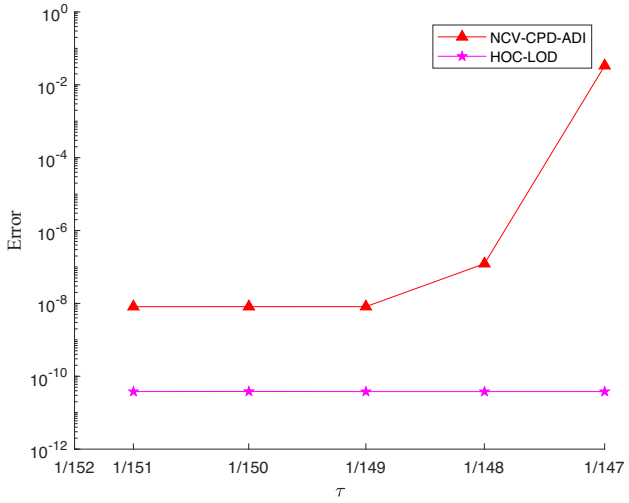

Fig. 1 The $\|e_h\|_\infty$ for various τ at $h = \pi/200$ at $T = 1$ for Problem 1

4.1 Problem 1

We discuss the 2D linear equation with variable wave speed [6]

$$\frac{\partial^2 u}{\partial t^2} = [1+\sin^2(x)+\sin^2(y)](\frac{\partial^2 u}{\partial x^2}+\frac{\partial^2 u}{\partial y^2}) + \left[3+2\sin^2(x)+2\sin^2(y)\right]e^{-t}\cos(x)\cos(y), (x, y, t) \in (0,\pi)^2\times(0, T],$$

with the initial conditions $u(x, y, 0) = \cos(x)\cos(y)$, $\frac{\partial u(x,y,0)}{\partial t} = -\cos(x)\cos(y)$ and boundary conditions $u(0,$

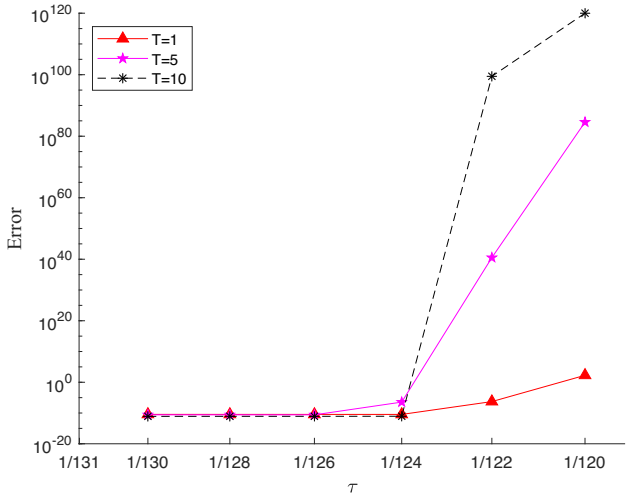

Fig. 2 The $\|e_h\|_\infty$ for different T and τ with $h = \pi/200$ by the HOC-LOD scheme for Problem 1

Table 2 The $\|e_h\|_\infty$ and $\|e_h\|_2$ for various h at $T = 1$ for Problem 2

h	ADI [21]($\tau = h^2$)		ADI [24]($\tau = h^2$)		HOC-LOD($\tau = h/3$)	
	$\|e_h\|_\infty$	$\|e_h\|_2$	$\|e_h\|_\infty$	$\|e_h\|_2$	$\|e_h\|_\infty$	$\|e_h\|_2$
1/2	3.220(-2)	1.507(-1)	3.506(-2)	1.615(-1)	1.665(-3)	5.721(-3)
1/4	2.503(-3)	1.097(-2)	2.509(-3)	1.106(-2)	1.272(-4)	3.505(-4)
1/8	1.624(-4)	7.038(-4)	1.622(-4)	7.050(-4)	8.091(-6)	2.208(-5)
1/16	1.030(-5)	4.426(-5)	1.031(-5)	4.428(-5)	5.174(-7)	1.391(-6)

$y, t) = -u(\pi, y, t) = e^{-t}\cos(y), u(x, 0, t) = -u(x, \pi, t) = e^{-t}\cos(x)$. The exact solution is $u(x, y, t) = e^{-t}\cos(x)\cos(y)$.

To confirm the advantages of the method of this paper, we take various h and τ at $T = 1$. Table 1 lists the $\|e_h\|_\infty$ and convergence orders given by the non constant velocity-compact Padé difference-ADI (NCV-CPD-ADI) scheme [6] and the presented HOC-LOD scheme. Compared with the NCV-CPD-ADI scheme [6], the HOC-LOD scheme shows smaller calculation errors and higher accuracy. Next, for this problem, we compare the stability condition ranges of the two schemes. The stability condition range of the scheme in Ref. [6] is $v_{\max}\lambda \le 0.7321$. Because of $v_{\max} = \sqrt{\max_{(x,y)\in[0,\pi]\times[0,\pi]}[1 + \sin^2(x) + \sin^2(y)]} = \sqrt{3}$, when $h = \frac{\pi}{200}$, the $\tau < \frac{0.7321\pi}{200\sqrt{3}} \approx 0.00663$ and $\frac{1}{150} < 0.00663 < \frac{1}{151}$. We take several values near $\frac{1}{150}$, these results are showed in Fig. 1. Figure 1 reflects when $\tau \ge \frac{1}{148}$, the $\|e_h\|_\infty$ of the scheme in Ref. [6] increases faster, then, it is divergent beyond the stability condition range, while that of the HOC-LOD scheme is still convergent. Therefore, the presented scheme maintains better stability than the scheme in Ref. [6] does. Then, when $h = \pi/200$, in Fig. 2, we further test the stability condition range of the presented scheme by calculating $\|e_h\|_\infty$. When the time T grows, $\tau \le \frac{1}{124}$, $v_{\max}\lambda \le 0.8892$, the presented scheme is convergent. When $\tau \ge \frac{1}{122}$, $v_{\max}\lambda \ge 0.9038$, the presented scheme is divergent. See Tables 10 and 11 in Appendix B for the corresponding data of Figs. 1 and 2.

4.2 Problem 2

Next, we consider the 2D sine-Gordon equation,

$$\frac{\partial^2 u}{\partial t^2} - v^2(x, y)\left(\frac{\partial^2 u}{\partial x^2} + \frac{\partial^2 u}{\partial y^2}\right) = f(u),\ (x, y, t) \in \Omega \times (0, T].$$

Firstly, we set $v^2(x, y) = 1$, $\Omega = (-7, 7)^2$ with the initial conditions $u(x, y, 0) = 4\arctan(e^{x+y})$, $\frac{\partial u}{\partial t}(x, y, 0) = \frac{-4e^{x+y}}{1+e^{2x+2y}}$ and boundary conditions $u(-7, y, t) = 4\arctan\left(e^{-7+y-t}\right)$, $u(7, y, t) = 4\arctan\left(e^{7+y-t}\right)$, $u(x, -7, t) = 4\arctan\left(e^{-7+x-t}\right)$, $u(x, 7, t) = 4\arctan\left(e^{7+x-t}\right)$. At this time, the exact solution is $u(x, y, t) = 4\arctan(e^{x+y-t})$ [19, 21, 24] and the nonlinear source term is $f(u) = -sin(u)$.

Table 2 compares the $\|e_h\|_2$ and $\|e_h\|_\infty$ given by the ADI scheme [21] with $\tau = h^2$, the ADI scheme [24] with $\tau = h^2$ and the HOC-LOD scheme with $\tau = h/3$. From Table 2, we can clearly see that the numerical solution of the presented scheme is more accurate than that of Refs. [21] and [24]. Moreover, because the HOC-LOD scheme adopts a relatively larger time step size, it only requires a small number of time steps to advance to a fixed time T, which can improve the computational efficiency. When $\tau = 0.01$, $h = 0.1$, Table 3 presents the $\|e_h\|_2$ and $\|e_h\|_\infty$ obtained by the ADI scheme [21], the localized method of approximate particular solutions (LMAPS) scheme [19] and the HOC-LOD scheme for different T. By comparing the results in Table 3, we find the HOC-LOD scheme is more accurate than the schemes in Refs. [21] and [19].

Table 3 The $\|e_h\|_\infty$ and $\|e_h\|_2$ with $\tau = 0.01$, $h = 0.1$ for different T for Problem 2

T	ADI [21]		LMAPS [19]		HOC-LOD	
	$\|e_h\|_\infty$	$\|e_h\|_2$	$\|e_h\|_\infty$	$\|e_h\|_2$	$\|e_h\|_\infty$	$\|e_h\|_2$
1	2.35(-4)	7.4(-4)	4.02(-4)	3.1(-3)	3.44(-6)	9.4(-6)
3	5.15(-4)	1.5(-3)	2.52(-4)	3.9(-3)	7.87(-6)	2.0(-5)
5	5.72(-4)	2.0(-3)	3.95(-4)	5.1(-3)	8.20(-6)	2.4(-5)
7	6.98(-4)	1.9(-3)	5.85(-4)	5.7(-3)	9.61(-6)	2.5(-5)

Table 4 The $\|e_h\|_\infty$, $\|e_h\|_2$, and $Order$ when $T = 1$, $\tau = 1.0e-05$ with various h by the HOC-LOD scheme for Problem 2

h	$\|e_h\|_\infty$	$Order$	$\|e_h\|_2$	$Order$
1/2	3.2804(-2)		3.2695(-2)	
1/4	1.8888(-3)	4.1183	1.8746(-3)	4.1244
1/8	1.1569(-4)	4.0291	1.1478(-4)	4.0296
1/16	7.5493(-6)	3.9378	7.4615(-6)	3.9433

Table 5 The $\|e_h\|_\infty$, $\|e_h\|_2$, and $Order$ when $T = 3$, $\tau/h = 0.2$ with various τ by the HOC-LOD scheme for Problem 2

τ	$\|e_h\|_\infty$	$Order$	$\|e_h\|_2$	$Order$
1/10	8.3111(-2)		8.2284(-2)	
1/20	4.7868(-3)	4.1179	4.7869(-3)	4.1034
1/30	9.6727(-4)	3.9440	9.5713(-4)	3.9700
1/40	3.2086(-4)	3.8357	3.1468(-4)	3.8667

Secondly, we set $v^2(x, y) = 1+0.1x+0.1y$, $\Omega = (0, 2)^2$ with the initial conditions $u(x, y, 0) = 0$, $\frac{\partial u}{\partial t}(x, y, 0) = \sin(\pi x)\sin(\pi y)$ and boundary conditions $u(0, y, t) = u(2, y, t) = u(x, 0, t) = u(x, 2, t) = 0$. At this time, the exact solution is $u(x, y, t) = t\sin(\pi x)\sin(\pi y)$ and the nonlinear source term is $f(u) = 2\pi^2 t(1 + 0.1x + 0.1y)\sin(\pi x)\sin(\pi y) + \sin[t\sin(\pi x)\sin(\pi y)] - \sin(u)$.

To test the space accuracy of the HOC-LOD scheme, we take different h at $T = 1$ and $\tau = 1.0e-05$, which means that the approximation error in time direction is negligible. Table 4 presents the $\|e_h\|_2$, $\|e_h\|_\infty$, and space convergence orders. It is obvious that the HOC-LOD scheme achieves fourth-order spatial convergence. Afterwards, to test the temporal accuracy of the HOC-LOD scheme, for different τ, we take $\frac{\tau}{h} = 0.2$ and $T = 3$, the $\|e_h\|_2$, $\|e_h\|_\infty$, and convergence orders are listed in Table 5, which display that the temporal accuracy of the presented scheme is fourth-order.

4.3 Problem 3

Consider the 2D sine-Gordon equation [18, 22],

$$\frac{\partial^2 u}{\partial t^2} - \left(\frac{\partial^2 u}{\partial x^2} + \frac{\partial^2 u}{\partial y^2}\right) = -\sin(u),\ (x, y, t) \in (-15, 15)^2 \times (0, T],$$

with initial conditions $u(x, y, 0) = 4\arctan(e^{3-\sqrt{x^2+y^2}})$, $\frac{\partial u}{\partial t}(x, y, 0) = 0$ and boundary conditions $u(-15, y, t) = u(15, y, t) = u(x, -15, t) = u(x, 15, t) = 0$. The exact solution of this problem is not available. The spatial grid size $h = 0.1$ and the temporal step size $\tau = 0.01$ are chosen to solve Problem 3.

Figure 3 describes wave field snapshots of $\sin\left(\frac{u^n}{2}\right)$ at different times. Figure 4 shows the corresponding contours. When $t = 0$, the soliton begins to shrink in Fig. 3(a). Subsequently, the solution begins to produce radiation and expands outward. When $t = 10.5s$, in Fig. 3(d), we can see that it forms a new soliton and begins a new phase of contraction. It can be clearly seen from Fig. 4 that in the whole simulation, the center of the soliton does not shift and there is no oscillation. These results are in agreement with those in Refs. [18, 22].

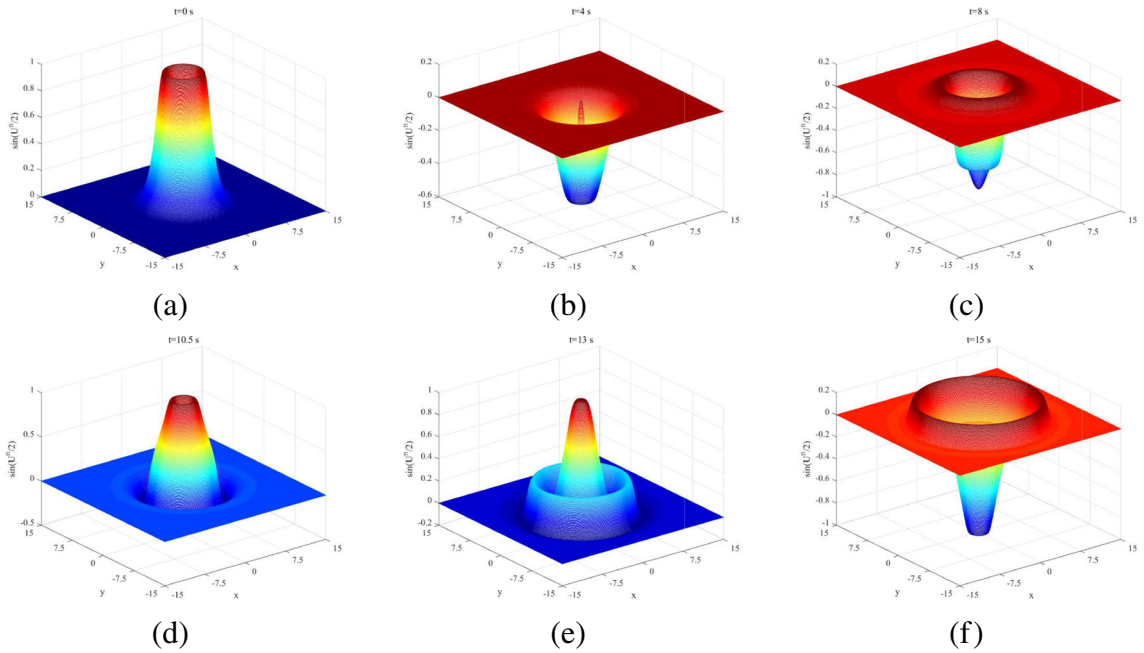

Fig. 3 Wave field snapshots of $\sin\left(\frac{u^n}{2}\right)$ at different times: **a** t=0s, **b** t=4s, **c** t=8s, **d** t=10.5s, **e** t=13s, **f** t=15s

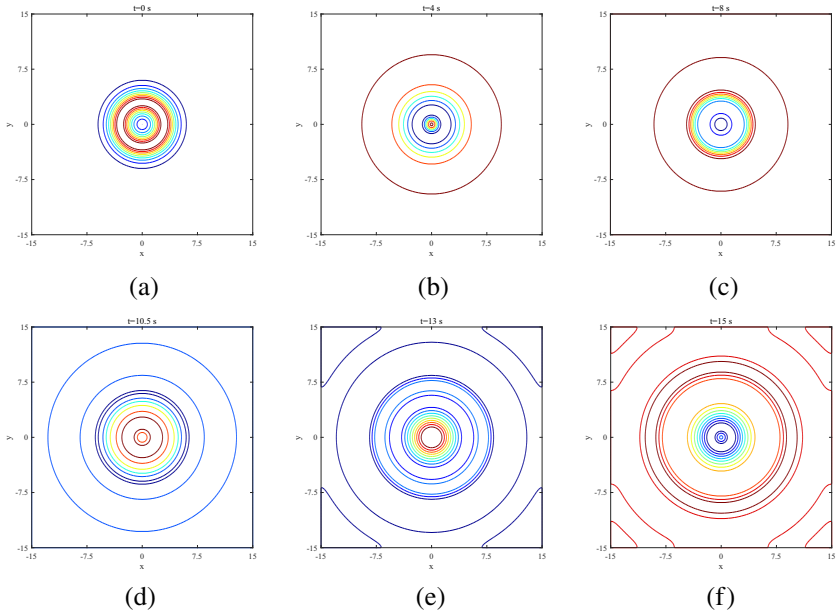

Fig. 4 The corresponding contours of $\sin\left(\frac{u^n}{2}\right)$: **a** t=0s, **b** t=4s, **c** t=8s, **d** t=10.5s, **e** t=13s, **f** t=15s

4.4 Problem 4

We discuss the 3D linear equation with variable wave speed [27]

$$\begin{aligned}\frac{\partial u^2}{\partial t^2} &= \left[1+\sin^2(x)+\sin^2(y)+\sin^2(z)\right]\left(\frac{\partial u^2}{\partial x^2}+\frac{\partial u^2}{\partial y^2}+\frac{\partial u^2}{\partial z^2}\right)\\ &+\left[4+3\sin^2(x)+3\sin^2(y)+3\sin^2(z)\right]e^{-t}\cos(x)\\ &\cos(y)\cos(z),\ (x,y,z,t)\in(0,\pi)^3\times(0,T],\end{aligned}$$

with the initial conditions $u(x,y,z,0) = \cos(x)\cos(y)\cos(z)$, $\frac{\partial u}{\partial t}(x,y,z,0) = -\cos(x)\cos(y)\cos(z)$ and boundary conditions $u(0,y,z,t) = -u(\pi,y,z,t) = e^{-t}\cos(y)\cos(z)$, $u(x,0,z,t) = -u(x,\pi,z,t) = e^{-t}\cos(x)\cos(z)$, $u(x,y,0,t) = -u(x,y,\pi,t) = e^{-t}\cos(x)\cos(y)$. The exact solution is $u(x,y,z,t) = e^{-t}\cos(x)\cos(y)\cos(z)$.

Table 6 is listed to test the accuracy of the HOC-LOD scheme by computing the $\|e_h\|_\infty$ and convergence orders with various h and τ at $T = 1$. It is clear that the results of the presented scheme are also more accurate than that of the ADI scheme [27]. Moreover, when the temporal step size τ decreases continuously, the accuracy increases gradually.

For this problem, $v_{\max} = \sqrt{\max_{(x,y,z)\in[0,\pi]\times[0,\pi]\times[0,\pi]}\left[1+\sin^2(x)+\sin^2(y)+\sin^2(z)\right]} = 2$, the stability condition range of the ADI scheme [27] is $v_{\max}\lambda \le 0.5770$. When $\frac{\tau}{h} = \frac{9}{10\pi} \approx 0.2865 \le 0.2885$, $v_{\max}\frac{\tau}{h} \le 0.5770$, the results in Table 7 display that the ADI scheme [27] and the HOC-LOD scheme are convergent. Then, when $\frac{\tau}{h} = \frac{19}{20\pi} \approx 0.3024 \ge 0.2885$, $v_{\max}\frac{\tau}{h} \ge 0.5770$, the results in the Table 8 reveal that the ADI scheme [27] is divergent, while the HOC-LOD scheme is still convergent. Thus, the stability condition of the presented scheme is better than that of the scheme in Ref. [27].

Table 6 The $\|e_h\|_\infty$ and $Order$ for different h and τ with $T = 1$ for Problem 4

	ADI [27]		HOC-LOD	
(h,τ)	$\|e_h\|_\infty$	$Order$	$\|e_h\|_\infty$	$Order$
$(\pi/16, 1/20)$	5.1391(-5)		3.1887(-7)	
$(\pi/32, 1/40)$	4.2849(-6)	3.5842	2.6995(-8)	3.5622
$(\pi/64, 1/80)$	3.9569(-7)	3.4368	1.8749(-9)	3.8478
$(\pi/128, 1/160)$	2.9088(-8)	3.7659	1.2241(-10)	3.9370

Table 7 The $\|e_h\|_\infty$ and $Order$ when $T = 1$, $v_{\max}\frac{\tau}{h} \le 0.5770$ with various h and τ for Problem 4

	ADI [27]		HOC-LOD	
(h,τ)	$\|e_h\|_\infty$	$Order$	$\|e_h\|_\infty$	$Order$
$(\pi/18, 1/20)$	3.3689(-5)		2.0973(-7)	
$(\pi/36, 1/40)$	2.7867(-6)	3.5842	1.7259(-8)	3.6031
$(\pi/54, 1/60)$	6.9049(-7)	3.4410	3.6503(-9)	3.8315
$(\pi/72, 1/80)$	2.7001(-8)	3.2638	1.1943(-9)	3.8836

Table 8 The $\|e_h\|_\infty$ and $Order$ when $T = 1$, $v_{\max}\frac{\tau}{h} \geq 0.5770$ with various h and τ for Problem 4

	ADI [27]		HOC-LOD	
(h, τ)	$\|e_h\|_\infty$	$Order$	$\|e_h\|_\infty$	$Order$
$(\pi/19, 1/20)$	8.5884(-5)		1.7724(-7)	
$(\pi/38, 1/40)$	1.1864(-5)	2.8557	1.4252(-8)	3.6365
$(\pi/57, 1/60)$	7.2660(-1)	-	2.9995(-9)	3.8436
$(\pi/76, 1/80)$	1.3165+006	-	9.7612(-10)	3.9023

In the end, to further study the stability condition range of the presented scheme, we choose $h = \pi/80$ to compute the $\|e_h\|_\infty$ with different T and τ. The computed results are listed in Fig. 5. When time T grows, we notice that $\tau \leq \frac{1}{69}$, $v_{\max}\lambda \leq 0.7381$, the presented scheme is convergent, while $\tau \geq \frac{1}{68}$, $v_{\max}\lambda \geq 0.7490$, the presented scheme is divergent. See Table 12 in Appendix B for the corresponding data of Fig. 5.

4.5 Problem 5

For the 3D sine-Gordon equation [23]

$$\frac{\partial^2 u}{\partial t^2} - \left(\frac{\partial^2 u}{\partial x^2} + \frac{\partial^2 u}{\partial y^2} + \frac{\partial^2 u}{\partial z^2}\right) = -\sin(u), (x, y, z, t) \in (0, 1)^3 \times (0, T],$$

with the initial conditions $u(x, y, z, 0) = 4\arctan(e^{x+y+z})$, $\frac{\partial u}{\partial t}(x, y, z, 0) = \frac{-4\sqrt{2}e^{x+y+z}}{1+e^{2x+2y+2z-2\sqrt{2}t}}$, the exact solution is $u(x, y, z, t) = 4\arctan(e^{x+y+z-\sqrt{2}t})$.

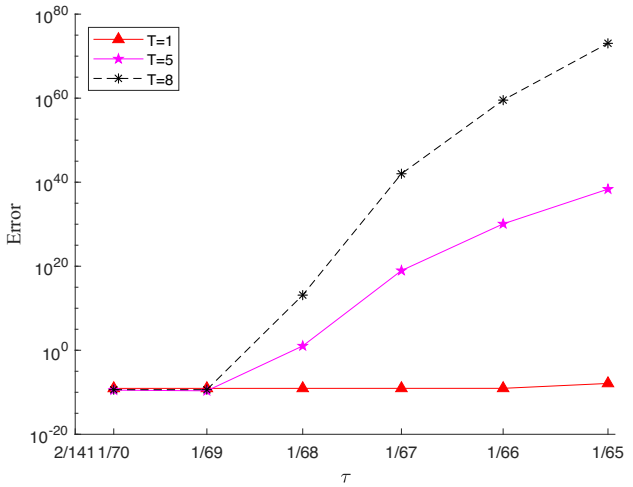

Fig. 5 The $\|e_h\|_\infty$ for different T and τ at $h = \pi/80$ by the HOC-LOD scheme for Problem 4

Table 9 The $\|e_h\|_\infty$ and $\|e_h\|_2$ when $T = 1, \tau = 1.0e-05$ with various h for Problem 5

	ADI-II [23]		HOC-LOD	
h	$\|e_h\|_\infty$	$\|e_h\|_2$	$\|e_h\|_\infty$	$\|e_h\|_2$
1/4	2.9411(-4)	1.0831(-4)	8.2089(-5)	3.1179(-5)
1/8	2.1060(-5)	6.6004(-6)	6.2612(-6)	1.9621(-6)
1/16	1.3195(-6)	4.0943(-7)	4.8655(-7)	1.4085(-7)

When $T = 1$, $\tau = 1.0e-5$ with various h, the $\|e_h\|_\infty$ and $\|e_h\|_2$ calculated by the ADI-II method [23] and the HOC-LOD method are listed in Table 9. From Table 9, it is easy to see our method is more accurate than that in Ref. [23]. To test the convergence order of the HOC-LOD scheme, in Fig. 6, we draw log-log plots for the $\|e_h\|_\infty$ and $\|e_h\|_2$. When $T = 0.1, \tau = 0.001$ at various h, the $\|e_h\|_\infty$ and $\|e_h\|_2$ obtained by the HOC-LOD method are plotted in Fig. 6(a). When $T = 1, h = 2\tau$ with various τ, the $\|e_h\|_\infty$ and $\|e_h\|_2$ are plotted in Fig. 6(b). From Fig. 6, it can be seen that the slope of the line of the the $\|e_h\|_\infty$ and $\|e_h\|_2$ are close to 4, which represents that the HOC-LOD scheme can converge to fourth-order in both time and space. See Tables 13 and 14 in Appendix B for the corresponding data of Fig. 6.

4.6 Problem 6

Example 6 is a 3D domain $[0m, 2km] \times [0m, 2km] \times [0m, 2km]$ model with a wave source [7]. The Ricker wavelet source that generates the wave is given by

$$f(x, y, z, t) = \delta(x - x_0, y - y_0, z - z_0)\Big[1 - 2\pi^2 f_p^2 \times (t - dr)^2\Big]e^{-\pi^2 f_p^2 (t-dr)^2},$$

where the centre of the domain is located at $(x_0, y_0, z_0) = (1000m, 1000m, 1000m)$. $f_p = 20Hz$ is the peak frequency. $dr = 2/f_p$ is the temporal delay that is used to ensure zero initial conditions. $\tau = 0.001s$, $v(x, y, z) = 2000m/s$. The exact solution is given by Hoop [37].

Firstly, the spatial grid size $h = 16m$ and $h = 8m$ are chosen to solve Example 6, respectively. The calculation results are shown in Fig. 7. As can be seen from Fig. 7, the smaller the grid size, the closer the calculated seismogram is to the exact solution, which means that the present scheme is highly accurate. Then, when we take the spatial grid size $h = 20m$, in Fig. 8, we draw wave field snapshots computed by the HOC-LOD scheme at $z = z_{max}/2$ for the model: (a) t=0.1s, (b) t=0.3s, (c) t=0.5s, (d) t=0.7s. Since the distance between

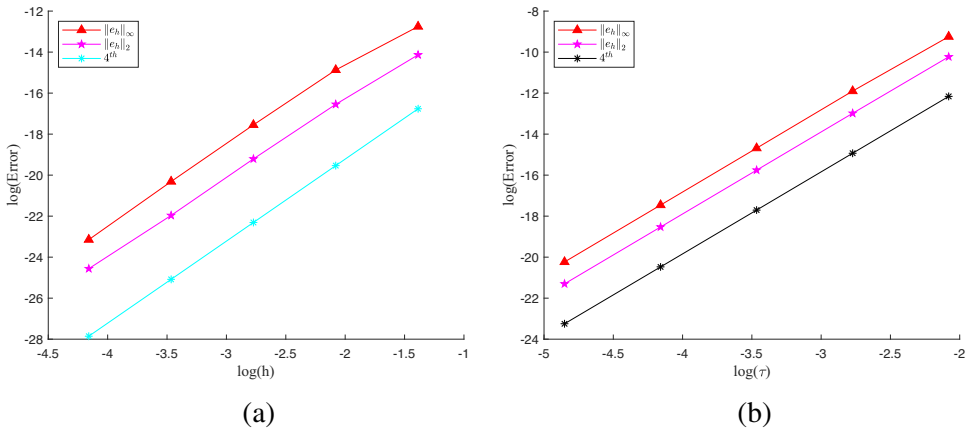

Fig. 6 Log-log plots for the $\|e_h\|_\infty$ and $\|e_h\|_2$ by the HOC-LOD scheme for Problem 4

the source and the rock area is $2000m - 1000m = 1000m$, the wave will reach the rock area at $t = \frac{1000m}{2000m/s} = 0.5$s. Therefore, when t=0.1s, t=0.3s and t=0.5s, the wave still forms a complete circle in Fig. 8(a)-(c). As time grows to t=0.7s, more reflection phenomenon around the boundary will be generated in Fig. 8(d), while there's still no reflection at the corners, since the distance from the source to the corner points are $1000^2 + 1000^2 = 1000\sqrt{2}m$, so when $t = \frac{1000\sqrt{2}m}{2000m/s} \approx 0.71$s, the wave will arrive the corners. The simulation results are consistent with the real physical process.

5 Conclusion

In this paper, we presented two high accurate implicit compact difference schemes based on the LOD method for solving the 2D and 3D nonlinear wave equations. The LOD technique was employed to split the high-dimensional nonlinear wave equations into several 1D equations. The fourth-order compact difference approximation formulas of the second-order derivatives were used to constructed implicit compact difference schemes with $O\left(\tau^4 + \tau^2 h^2 + h^4\right)$. Through the numerical experiments of linear wave equations with variable coefficient and nonlinear sine-Gordon equations, we validated the presented schemes are fourth-order accuracy and the stability conditions of the 2D and 3D problems are $v_{\max}\lambda \in (0, 0.8944]$ and $v_{\max}\lambda \in (0, 0.7385]$, respectively.

In recent years, several researchers have proposed numerical methods for solving the nonlinear coupled wave equations and nonlinear fourth-order equations [38–40]. To generalize

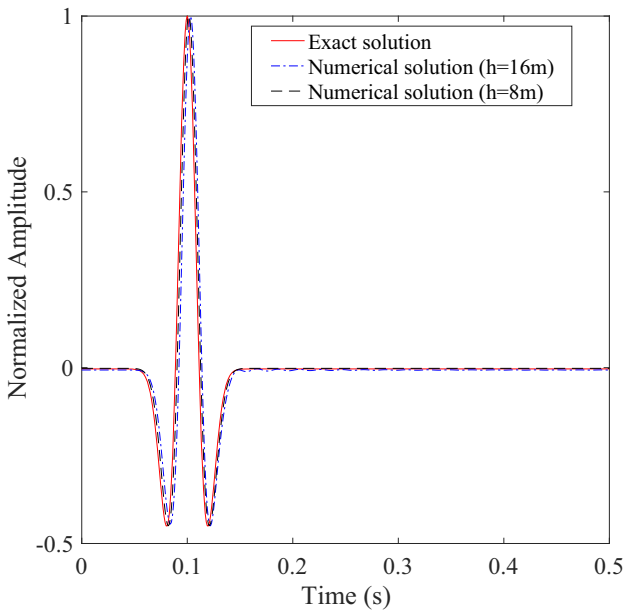

Fig. 7 Normalized waveforms computed by using different grid sizes at $(1000m, 1000m, 1000m)$

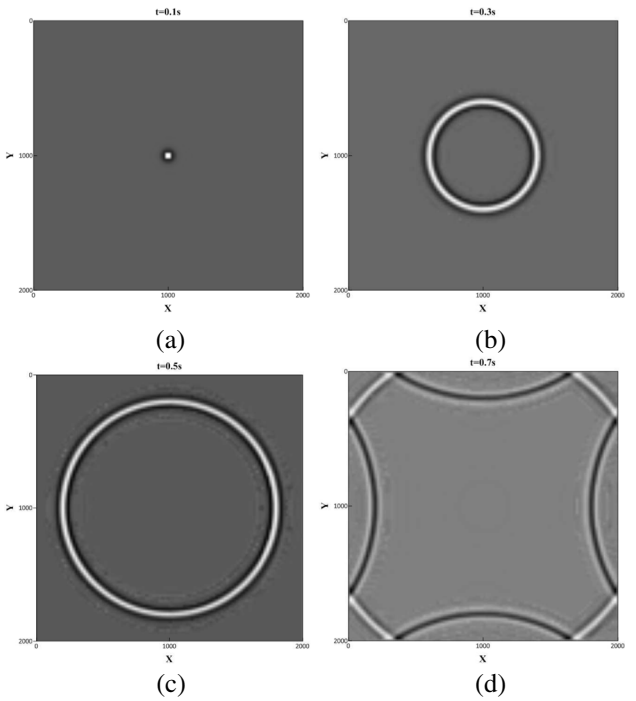

Fig. 8 Wave fields snapshots at $z = z_{max}/2$: **a** t=0.1s, **b** t=0.3s, **c** t=0.5s, **d** t=0.7s

the presented method to this kind of partial differential equations is our ongoing research work.

Appendix A

Lemma 1 [36] *The sufficient and necessary condition for the roots of the quadratic equation $\delta^2 - b_1\delta - c_1 = 0$ with real coefficients to be less than or equal to 1 is $|c_1| \le 1, |b_1| \le 1 - c_1$.*

Theorem 2 *The scheme is stable if*

$$\max_{1\le i,j,k\le N}|\frac{v_{i,j,k}\cdot\tau}{h}| = v_{\max}\lambda \le 0.7385,$$

in which, $v_{\max} = \max_{1\le i,j,k\le N}|v_{i,j,k}|$.

Proof Letting $u^n_{i,j,k} = \eta^n e^{I\sigma_1 x_i} e^{I\sigma_2 y_j} e^{I\sigma_3 z_k}$, $u^{n+\frac{1}{3}}_{i,j,k} = \eta^{n+\frac{1}{3}} e^{I\sigma_1 x_i} e^{I\sigma_2 y_j} e^{I\sigma_3 z_k}$, $u^{n-\frac{1}{3}}_{i,j,k} = \eta^{n-\frac{1}{3}} e^{I\sigma_1 x_i} e^{I\sigma_2 y_j} e^{I\sigma_3 z_k}$, $\max_{1\le i,j,k\le N} v^2_{i,j,k} = a$, and multiplying by a on the both sides of Eq. (45), we have

$$\begin{aligned}
&\left(\frac{5}{6}+\frac{a\lambda^2}{18}\right)\eta^{n+\frac{1}{3}} e^{I\sigma_1 x_i} e^{I\sigma_2 y_j} e^{I\sigma_3 z_k}\\
&+\left(\frac{1}{12}-\frac{a\lambda^2}{36}\right)\eta^{n+\frac{1}{3}}\left(e^{I\sigma_1 x_{i+1}}+e^{I\sigma_1 x_{i-1}}\right) e^{I\sigma_2 y_j} e^{I\sigma_3 z_k}\\
=&\left(\frac{5}{3}-\frac{5a\lambda^2}{9}\right)\eta^{n} e^{I\sigma_1 x_i} e^{I\sigma_2 y_j} e^{I\sigma_3 z_k}\\
&+\left(\frac{1}{6}+\frac{5a\lambda^2}{18}\right)\eta^{n}\left(e^{I\sigma_1 x_{i+1}}+e^{I\sigma_1 x_{i-1}}\right) e^{I\sigma_2 y_j} e^{I\sigma_3 z_k}\\
&-\left(\frac{5}{6}+\frac{a\lambda^2}{18}\right)\eta^{n-\frac{1}{3}} e^{I\sigma_1 x_i} e^{I\sigma_2 y_j} e^{I\sigma_3 z_k}\\
&-\left(\frac{1}{12}-\frac{a\lambda^2}{36}\right)\eta^{n-\frac{1}{3}}\left(e^{I\sigma_1 x_{i+1}}+e^{I\sigma_1 x_{i-1}}\right) e^{I\sigma_2 y_j} e^{I\sigma_3 z_k}.
\end{aligned} \tag{A-1}$$

By $e^{\pm I\sigma h} = \cos\sigma h \pm I\sin\sigma h$, we get

$$\begin{aligned}
&\left(\frac{5}{6}+\frac{a\lambda^2}{18}\right)\eta^{n+\frac{1}{3}} + 2\cos\sigma_1 h\left(\frac{1}{12}-\frac{a\lambda^2}{36}\right)\eta^{n+\frac{1}{3}}\\
=&\left(\frac{5}{3}-\frac{5a\lambda^2}{9}\right)\eta^{n} + 2\cos\sigma_1 h\left(\frac{1}{6}+\frac{5a\lambda^2}{18}\right)\eta^{n}\\
&-\left(\frac{5}{6}+\frac{a\lambda^2}{18}\right)\eta^{n-\frac{1}{3}} - 2\cos\sigma_1 h\left(\frac{1}{12}-\frac{a\lambda^2}{36}\right)\eta^{n-\frac{1}{3}}.
\end{aligned} \tag{A-2}$$

Letting $\varepsilon^{n+\frac{1}{3}} = \eta^n$, $\varepsilon^n = \eta^{n-\frac{1}{3}}$, Eq. (A-2) is written in matrix form

$$\begin{aligned}
&\begin{bmatrix}\frac{5}{6}+\frac{a\lambda^2}{18}+\left(\frac{1}{6}-\frac{a\lambda^2}{18}\right)\cos\sigma_1 h & 0\\ 0 & 1\end{bmatrix}\begin{bmatrix}\eta^{n+\frac{1}{3}}\\ \varepsilon^{n+\frac{1}{3}}\end{bmatrix}\\
=&\begin{bmatrix}\frac{5}{3}-\frac{5a\lambda^2}{9}+\left(\frac{1}{3}+\frac{5a\lambda^2}{9}\right)\cos\sigma_1 h & -\left(\frac{5}{6}+\frac{a\lambda^2}{18}\right)-\left(\frac{1}{6}-\frac{a\lambda^2}{18}\right)\cos\sigma_1 h\\ 1 & 0\end{bmatrix}\begin{bmatrix}\eta^{n}\\ \varepsilon^{n}\end{bmatrix}.
\end{aligned} \tag{A-3}$$

Letting $U^n = (\eta^n, \varepsilon^n)^T$ and substituting it into Eq. (A-3) to get

$$\begin{aligned}
&\begin{bmatrix}\frac{5}{6}+\frac{a\lambda^2}{18}+\left(\frac{1}{6}-\frac{a\lambda^2}{18}\right)\cos\sigma_1 h & 0\\ 0 & 1\end{bmatrix}U^{n+\frac{1}{3}}\\
=&\begin{bmatrix}\frac{5}{3}-\frac{5a\lambda^2}{9}+\left(\frac{1}{3}+\frac{5a\lambda^2}{9}\right)\cos\sigma_1 h & -\left(\frac{5}{6}+\frac{a\lambda^2}{18}\right)-\left(\frac{1}{6}-\frac{a\lambda^2}{18}\right)\cos\sigma_1 h\\ 1 & 0\end{bmatrix}U^{n}.
\end{aligned} \tag{A-4}$$

Similarly, Eqs. (46) and (47) can be treated as

$$\begin{aligned}
&\begin{bmatrix}\frac{5}{6}+\frac{a\lambda^2}{18}+\left(\frac{1}{6}-\frac{a\lambda^2}{18}\right)\cos\sigma_2 h & 0\\ 0 & 1\end{bmatrix}U^{n+\frac{2}{3}}\\
=&\begin{bmatrix}\frac{5}{3}-\frac{5a\lambda^2}{9}+\left(\frac{1}{3}+\frac{5a\lambda^2}{9}\right)\cos\sigma_2 h & -\left(\frac{5}{6}+\frac{a\lambda^2}{18}\right)-\left(\frac{1}{6}-\frac{a\lambda^2}{18}\right)\cos\sigma_2 h\\ 1 & 0\end{bmatrix}U^{n+\frac{1}{3}},
\end{aligned} \tag{A-5}$$

and

$$\begin{aligned}
&\begin{bmatrix}\frac{5}{6}+\frac{a\lambda^2}{18}+\left(\frac{1}{6}-\frac{a\lambda^2}{18}\right)\cos\sigma_3 h & 0\\ 0 & 1\end{bmatrix}U^{n+1}\\
=&\begin{bmatrix}\frac{5}{3}-\frac{5a\lambda^2}{9}+\left(\frac{1}{3}+\frac{5a\lambda^2}{9}\right)\cos\sigma_3 h & -\left(\frac{5}{6}+\frac{a\lambda^2}{18}\right)-\left(\frac{1}{6}-\frac{a\lambda^2}{18}\right)\cos\sigma_3 h\\ 1 & 0\end{bmatrix}U^{n+\frac{2}{3}}.
\end{aligned} \tag{A-6}$$

Substituting Eqs. (A-4)-(A-5) into Eq. (A-6), the error propagation matrix is

$$G = \begin{bmatrix}-\frac{B_x}{A_x}-\frac{B_z}{A_z}+\frac{B_xB_yB_z}{A_xA_yA_z} & 1-\frac{B_yB_z}{A_yA_z}\\ \frac{B_xB_y}{A_xA_y}-1 & -\frac{B_y}{A_y}\end{bmatrix},$$

in which,

$$\begin{aligned}
A_x &= \frac{5}{6}+\frac{a\lambda^2}{18}+\left(\frac{1}{6}-\frac{a\lambda^2}{18}\right)\cos\sigma_1 h,\\
A_y &= \frac{5}{6}+\frac{a^2\lambda^2}{18}+\left(\frac{1}{6}-\frac{a\lambda^2}{18}\right)\cos\sigma_2 h,\\
A_z &= \frac{5}{6}+\frac{a\lambda^2}{18}+\left(\frac{1}{6}-\frac{a\lambda^2}{18}\right)\cos\sigma_3 h,\\
B_x &= \frac{5}{3}-\frac{5a\lambda^2}{9}+\left(\frac{1}{3}+\frac{5a\lambda^2}{9}\right)\cos\sigma_1 h,\\
B_y &= \frac{5}{3}-\frac{5a\lambda^2}{9}+\left(\frac{1}{3}+\frac{5a\lambda^2}{9}\right)\cos\sigma_2 h,\\
B_z &= \frac{5}{3}-\frac{5a\lambda^2}{9}+\left(\frac{1}{3}+\frac{5a\lambda^2}{9}\right)\cos\sigma_3 h.
\end{aligned}$$

The characteristic equation can be obtained by

$$|\mu I - G| = \mu^2 + \left(\frac{B_x}{A_x} + \frac{B_y}{A_y} + \frac{B_z}{A_z} - \frac{B_x B_y B_z}{A_x A_y A_z}\right)\mu + 1 = 0.$$

According to the Lemma 1, when $|b_1| = |\frac{B_x B_y B_z}{A_x A_y A_z} - \left(\frac{B_x}{A_x} + \frac{B_y}{A_y} + \frac{B_z}{A_z}\right)| \le 2$, the scheme is stable.

Because $\frac{B_x}{A_x}$, $\frac{B_y}{A_y}$ and $\frac{B_z}{A_z}$ have the same range of values, thus, either $-2 \le \frac{B_x}{A_x}, \frac{B_y}{A_y}, \frac{B_z}{A_z} \le -1$ or $-1 \le \frac{B_x}{A_x}, \frac{B_y}{A_y}, \frac{B_z}{A_z} \le 1$ or $1 \le \frac{B_x}{A_x}, \frac{B_y}{A_y}, \frac{B_z}{A_z} \le 2$, the scheme is stable. Here, we only analyze the value range of $\frac{B_x}{A_x}$.

Letting $\cos \sigma_1 h = \theta, \theta \in [-1, 1]$, we assume that

$$G(\theta) = \frac{B_x}{A_x} = \frac{\frac{1}{3}(5+\theta) + \frac{5a\lambda^2}{9}(\theta - 1)}{\frac{1}{6}(5+\theta) + \frac{a\lambda^2}{18}(1-\theta)},$$

$G(\theta)$ is an increasing function, the value range of the function $G(\theta)$ is $\left[\frac{12-10a\lambda^2}{6+a\lambda^2}, 2\right]$. Due to either $-2 \le G(\theta) \le -1$ or $-1 \le G(\theta) \le 1$ or $1 \le G(\theta) \le 2$, the scheme is stable. So, when $1 \le \frac{12-10a\lambda^2}{6+a\lambda^2} \le 2$, i.e., $a\lambda^2 \le \frac{6}{11}$, the scheme is stable.

In summary, when $a\lambda^2 \le \frac{6}{11}$, i.e., $\upsilon_{\max}\lambda = \sqrt{a}\lambda \le 0.7385$, the scheme is stable. □

Appendix B

Table 10 The $\|e_h\|_\infty$ for various τ at $h = \pi/200$ at $T = 1$ for Problem 1

τ	NCV-CPD-ADI [6]	HOC-LOD
1/151	8.1293(-9)	3.8002(-11)
1/150	8.1398(-9)	3.8276(-11)
1/149	8.1505(-9)	3.7950(-11)
1/148	1.2298(-7)	3.7940(-11)
1/147	0.03347	3.7986(-11)

Table 11 The $\|e_h\|_\infty$ for various T and τ with $h = \pi/200$ by the HOC-LOD scheme for Problem 1

τ	$\upsilon_{\max}\lambda$	$T = 1$	$T = 5$	$T = 10$
1/160	0.6892	3.8687(-11)	2.8686(-11)	6.8250(-12)
1/150	0.7351	3.8276(-11)	2.8352(-11)	6.8505(-12)
1/140	0.7876	3.7468(-11)	2.7555(-11)	7.6552(-12)
1/130	0.8482	3.5921(-11)	2.6263(-11)	8.1260(-12)
1/128	0.8615	3.5644(-11)	2.6018(-11)	8.4228(-12)
1/126	0.8751	3.5128(-11)	2.5609(-11)	8.4245(-12)
1/124	0.8892	3.4984(-11)	3.5424(-11)	8.9238(-12)
1/122	0.9038	5.2233(-7)	3.4157+040	2.9986+099
1/120	0.9189	1.8347+002	3.8697+084	overflow

Table 12 The $\|e_h\|_\infty$ for different T and τ at $h = \pi/80$ by the HOC-LOD scheme for Problem 4

τ	$\upsilon_{\max}\lambda$	$T = 1$	$T = 5$	$T = 8$
1/100	0.5093	7.8389(-10)	3.2381(-10)	3.5742(-10)
1/90	0.5659	7.9199(-10)	3.2153(-10)	3.6467(-10)
1/80	0.6366	8.0817(-10)	3.2139(-10)	3.7914(-10)
1/70	0.7276	8.4230(-10)	3.2337(-10)	4.1152(-10)
1/69	0.7381	8.4763(-10)	3.2388(-10)	4.1710(-10)
1/68	0.7490	8.5345(-10)	1.0672+001	1.3667+013
1/67	0.7601	8.5992(-10)	9.1963+018	1.0013+042
1/66	0.7717	8.6688(-10)	1.2019+030	3.4956+059
1/65	0.7835	1.2687(-8)	2.2293+038	1.1351+073

Table 13 The $\|e_h\|_\infty$ and $\|e_h\|_2$ when $T = 0.1$, $\tau = 0.001$ with various h by the HOC-LOD scheme for Problem 5

h	$\|e_h\|_\infty$	$\|e_h\|_2$
1/4	2.8898(-6)	7.2716(-7)
1/8	3.4833(-7)	6.5119(-8)
1/16	2.3899(-8)	4.5502(-9)
1/32	1.5071(-9)	2.8908(-10)
1/64	8.8603(-11)	2.1544(-11)

Table 14 The $\|e_h\|_\infty$ and $\|e_h\|_2$ when $T = 1, h = 2\tau$ with various τ by the HOC-LOD scheme for Problem 5

τ	$\|e_h\|_\infty$	$\|e_h\|_2$
1/8	9.6294(-5)	3.6073(-5)
1/16	6.7875(-6)	2.2952(-6)
1/32	4.1921(-7)	1.4369(-7)
1/64	2.6160(-8)	8.9755(-9)
1/128	1.6295(-9)	5.6077(-10)

Acknowledgements This work is partially supported by National Natural Science Foundation of China (12161067, 12001015, 12261067), National Natural Science Foundation of Ningxia (2022AAC02023), National Youth Top-notch Talent Support Program of Ningxia, and the First Class Discipline Construction Project in Ningxia Universities: Mathematics.

Data Availability The data that support this study are available from the corresponding author on reasonable request.

Declarations

Conflict of interest The authors declare no potential conflict of interests.

References

1. Robertsson, J., Blanch, J., Nihei, K., Tromp, J.: Numerical modeling of seismic wave propagation. Society of Exploration Geophysicists (2012)
2. Moczo, P., Kristek, J., Galis, M.: The finite-difference modelling of earthquake motions: Waves and ruptures. Cambridge University Press. Geological Magazine (2014)
3. Li, L., Tan, J., Zhang, D., et al.: FD wave 3D: a MATLAB solver for the 3D anisotropic wave equation using the finite-difference method. Comput. Geosci. **25**, 1565–1578 (2021)
4. Wang, Z., Li, J., Wang, B., Xu, Y., Chen, X.: A new central compact finite difference scheme with high spectral resolution for acoustic wave equation. J. Comput. Phys. **366**, 191–206 (2018)
5. Abdulkadir, Y.: Comparison of finite difference schemes for the wave equation based on dispersion. J. Appl. Math. Phys. **3**, 1544–1562 (2015)
6. Liao, W., Yong, P., Dastour, H., Huang, J.: Efficient and accurate numerical simulation of acoustic wave propagation in a 2D heterogeneous media. Appl. Math. Comput. **321**, 385–400 (2018)
7. Liao, W.: On the dispersion, stability and accuracy of a compact higher-order finite difference scheme for 3D acoustic wave equation. J. Comput. Appl. Math. **270**, 571–583 (2014)
8. Fairweather, B., Kastner, R.: Finite difference time domain dispersion reduction schemes. J. Comput. Phys. **221**, 422–438 (2007)
9. Yang, D., Wang, L.: A split-step algorithm with effectively suppressing the numerical dispersion for 3D seismic propagation modeling. Bull. Seismol. Soc. Am. **100**, 1470–1484 (2010)
10. Yang, D., Tong, P., Deng, X.: A central difference method with low numerical dispersion for solving the scalar wave equation. Geophys. Prospect. **60**, 885–905 (2012)
11. Liu, Y., Sen, M.: A new time space domain high-order finite-difference method for the acoustic wave equation. J. Comput. Phys. **228**, 8779–8806 (2009)
12. Feo, F., Jordan, J., Rojas, O., Otero, B., Rodriguez, R.: A new mimetic scheme for the acoustic wave equation. J. Comput. Appl. Math. **295**, 2–12 (2016)
13. Jiwari, R., Pandit, S., Mittal, R.: Numerical simulation of two-dimensional sine-Gordon solitons by differential quadrature method. Comput. Phys. Commun. **183**, 600–616 (2012)
14. Torberntsson, K., Stiernström, V., Mattsson, K., Dunham, E.: A finite difference method for earthquake sequences in poroelastic solids. Comput. Geosci. 22, 1351-1370 (2018)
15. Sheen, D., Tuncay, K., Baag, C., Ortoleva, P.: Parallel implementation of a velocity-stress staggered-grid finite-difference method for 2-D poroelastic wave propagation. Comput. Geosci. **32**, 1182–1191 (2006)
16. Li, D., Sun, W.: Linearly implicit and high-order energy-conserving schemes for nonlinear wave equations. J. Sci. Comput. **83**, 65 (2020)
17. Bratsos, A.: A modified predictor-corrector scheme for the two-dimensional sine-Gordon equation. Numerical Algorithms **43**, 295–308 (2006)
18. Liu, C., Wu, X.: Arbitrarily high-order time-stepping schemes based on the operator spectrum theory for high-dimensional nonlinear Klein-Gordon equations. J. Comput. Phys. **340**, 243–275 (2017)
19. Su, L.: Numerical solution of two-dimensional nonlinear sine-Gordon equation using localized method of approximate particular solutions. Eng. Anal. Boundary Elem. **108**, 95–107 (2019)
20. Hou, B., Liang, D.: The energy-preserving time high-order AVF compact finite difference scheme for nonlinear wave equations in two dimensions. Appl. Numer. Math. **170**, 298–320 (2021)
21. Cui, M.: High order compact alternating direction implicit method for the generalized sine-Gordon equation. J. Comput. Appl. Math. **235**, 837–849 (2010)
22. Deng, D., Liang, D.: The time fourth-order compact ADI methods for solving two-dimensional nonlinear wave equations. Appl. Math. Comput. **329**, 188–209 (2018)
23. Deng, D.: Unified compact ADI methods for solving nonlinear viscous and nonviscous wave equations. Chin. J. Phys. **56**, 2897–2915 (2018)
24. Deng, D., Zhang, C.: A new fourth-order numerical algorithm for a class of nonlinear wave equations. Appl. Numer. Math. **62**, 1864–1879 (2012)
25. Peaceman, D., Rachford, H.: The numerical solution of parabolic and elliptic differential equations. J. Soc. Ind. Appl. Math. **3**, 28–41 (1955)
26. Deng, D., Zhang, C.: A family of new fourth-order solvers for a nonlinear damped wave equation. Comput. Phys. Commun. **184**, 86–101 (2013)
27. Li, K., Liao, W., Lin, Y.: A compact high-order alternating direction implicit method for three-dimensional acoustic wave equation with variable coefficient. J. Comput. Appl. Math. **361**, 113–129 (2019)
28. Zhang, W., Tong, L., Chung, E.: A new high accuracy locally one-dimensional scheme for the wave equation. J. Comput. Appl. Math. **236**, 1343–4353 (2011)
29. Zhang, W., Jiang, J.: A new family of fourth-order locally one-dimensional scheme for the three-dimensional wave equation. J. Comput. Appl. Math. **322**, 130–147 (2017)
30. Yun, N., Sun, C., Sim, C.: An optimal nearly analytic splitting method for solving 2D acoustic wave equations. J. Appl. Geophys. **177**, 104029 (2020)
31. Sim, C., Sun, C., Yun, N.: A nearly analytic symplectic partitioned Runge-Kutta method based on a locally one-dimensional technique for solving two-dimensional acoustic wave equations. Geophys. Prospect. **68**, 1253–1269 (2020)
32. Zhang, W.: A new family of fourth-order locally one-dimensional schemes for the 3D elastic wave equation. J. Comput. Appl. Math. **348**, 246–260 (2018)
33. Dehghan, M., Shokri, A.: A numerical method for the one-dimensional nonlinear sine-Gordon equation using collocation and radial basis functions. Numerical Methods for Partial Differential Equations **24**, 687–698 (2008)
34. Hirsh, R.: Higher order accurate difference solutions of fluid mechanics problem by a compact differencing technique. J. Comput. Phys. **19**, 90–109 (1975)
35. Samarskii, A.: Local one-dimensional difference schemes for multi-dimensional hyperbolic equations in an arbitrary region. USSR Comput. Math. Math. Phys. **4**, 21–35 (1964)
36. Yang, D.: Iterative Solution for Large Linear System. Academic Press, New York (1991)
37. Hoop, A.: A modification of Cagniards method for solving seismic pulse problems. Appl. Sci. Res. **8**, 349–356 (1960)
38. Zhang, G.: Two conservative and linearly-implicit compact difference schemes for the nonlinear fourth-order wave equation. Appl. Math. Comput. **401**, 126055 (2021)
39. Deng, D., Wu, Q.: Error estimations of the fourth-order explicit Richardson extrapolation method for two-dimensional nonlinear coupled wave equations. Comput. Appl. Math. **41**, 3 (2022)
40. Hashemi, M.: Numeical study of the one-dimensional coupled nonlinear sine-Gordon equations by a novel geometric meshless method. Engineering with Computers **37**, 3397–3407 (2021)